

AWARD NUMBER: W81XWH-18-1-0519
PC170821

TITLE: Early Detection of Castration-Resistant Prostate Cancer by Assessing Interactions between Circulating Tumor Cells and Accompanying Immune Cells

PRINCIPAL INVESTIGATOR: Tim H.M. Huang, PhD.

CONTRACTING ORGANIZATION: The University of Texas Health Science Center at San Antonio

REPORT DATE: September 2021

TYPE OF REPORT: Annual

PREPARED FOR: U.S. Army Medical Research and Development Command
Fort Detrick, Maryland 21702-5012

DISTRIBUTION STATEMENT: Approved for Public Release;
Distribution Unlimited

The views, opinions and/or findings contained in this report are those of the author(s) and should not be construed as an official Department of the Army position, policy or decision unless so designated by other documentation.

REPORT DOCUMENTATION PAGE

Form Approved
OMB No. 0704-0188

Public reporting burden for this collection of information is estimated to average 1 hour per response, including the time for reviewing instructions, searching existing data sources, gathering and maintaining the data needed, and completing and reviewing this collection of information. Send comments regarding this burden estimate or any other aspect of this collection of information, including suggestions for reducing this burden to Department of Defense, Washington Headquarters Services, Directorate for Information Operations and Reports (0704-0188), 1215 Jefferson Davis Highway, Suite 1204, Arlington, VA 22202-4302. Respondents should be aware that notwithstanding any other provision of law, no person shall be subject to any penalty for failing to comply with a collection of information if it does not display a currently valid OMB control number. PLEASE DO NOT RETURN YOUR FORM TO THE ABOVE ADDRESS.

1. REPORT DATE 09/14/2021		2. REPORT TYPE Annual		3. DATES COVERED 08/15/2020-08/14/2021	
4. TITLE AND SUBTITLE Early Detection of Castration-Resistant Prostate Cancer by Assessing Interactions between Circulating Tumor Cells and Accompanying Immune Cells				5a. CONTRACT NUMBER W81XWH1810519	
				5b. GRANT NUMBER PC170821	
				5c. PROGRAM ELEMENT NUMBER	
6. AUTHOR(S) Tim Hui-Ming Huang, PhD Maria Gaczynska, PhD Pawel Osmulski, PhD E-Mail: huangt3@uthscsa.edu				5d. PROJECT NUMBER	
				5e. TASK NUMBER	
				5f. WORK UNIT NUMBER	
7. PERFORMING ORGANIZATION NAME(S) AND ADDRESS(ES) The University of Texas Health Science center at San Antonio Office of Sponsored Programs 7703 Floyd Curl Drive, MC 7828 San Antonio, Texas 78229-3900				8. PERFORMING ORGANIZATION REPORT NUMBER	
9. SPONSORING / MONITORING AGENCY NAME(S) AND ADDRESS(ES) U.S. Army Medical Research and Development Command Fort Detrick, Maryland 21702-5012				10. SPONSOR/MONITOR'S ACRONYM(S)	
				11. SPONSOR/MONITOR'S REPORT NUMBER(S)	
12. DISTRIBUTION / AVAILABILITY STATEMENT Approved for Public Release; Distribution Unlimited					
13. SUPPLEMENTARY NOTES					
14. ABSTRACT Prostate cancer is the most frequent diagnosed cancer in men. In majority of "castration sensitive" patients proliferation of cancer cells depends on supply of androgen and can be attenuated by the androgen deprivation therapy (ADT). Unfortunately, many patients develop "castration resistance" (CR), when the tumor growth and metastatic spread continue despite ADT. For effective second-line therapy the resistance needs to be detected early. Circulating tumor cells (CTCs) that can be isolated from the standard blood sample are considered "seeds of metastasis". We postulate that mechanical and immunochemical profiling of CTCs and accompanying immune cells provide clues about CTCs aggressiveness and the risk of CR. Our specific aims call for determining the role of (1) epithelial-mesenchymal transition (EMT) and (2) interactions with circulating macrophages in survival-promoting mechanical fitness of CTCs. Combining the cell culture studies with profiling of CTCs will lead to (3) construction of predictive model for early CR detection. In the third reporting period we completed a majority of tasks in accordance with the statement of work. The exception is patients' accrual, slowed down by the pandemic. The project now enters NCE phase to finish the collection and analysis of patients' samples. The outcomes for now include a paper published in Cancer research.					
15. SUBJECT TERMS androgen deprivation therapy, atomic force microscopy, castration resistance, castration sensitivity, circulating tumor cells, cultured cells, epithelial-mesenchymal transition					
16. SECURITY CLASSIFICATION OF:			17. LIMITATION OF ABSTRACT	18. NUMBER OF PAGES	19a. NAME OF RESPONSIBLE PERSON
a. REPORT	b. ABSTRACT	c. THIS PAGE			USAMRDC
Unclassified	Unclassified	Unclassified	Unclassified	39	19b. TELEPHONE NUMBER (include area code)

Table of Contents

	<u>Page</u>
1. Introduction.....	04
2. Keywords.....	05
3. Key Research Accomplishments.....	6-19
Major goals of the project.....	6-8
Accomplishments under these goals.....	8-18
Training/professional development opportunities.....	18-19
Results dissemination.....	19
Future plans.....	19
4. Impact.....	20
5. Changes/Problems.....	21
6. Products.....	21
7. Participants.....	21-23
8. Special Reporting Requirements.....	24
9. Appendices.....	25-40

1. Introduction

Prostate cancer (PCa) is the most frequently diagnosed cancer in men. In majority of “castration sensitive” patients proliferation of cancer cells depends on supply of androgen and can be attenuated by the androgen deprivation therapy (ADT). Unfortunately, many patients develop “castration resistance” (CR), when the tumor growth and metastatic spread continue despite ADT. For effective second-line therapy that saves lives and improves life quality the resistance needs to be detected early. To reach the goal of early detection we propose to test properties of rare cells that are responsible for spreading metastasis. These circulating tumor cells (CTCs) are shed from the primary tumor or metastatic lesions and can be isolated from the standard blood sample are considered “seeds of metastasis”. Majority of CTCs die, however the surviving “aggressive” cells travel with blood, undergo epithelial-to-mesenchymal transition (EMT), extravasate and start secondary tumor growth in distant organs. Since CTCs have to escape from the tumor and then survive in the turbulent blood stream, they have to be mechanically fit. Indeed, we found in retrospective studies that CTCs obtained from CR patients are much softer, deformable and more adhesive than CTCs from CS patients. CTCs are often accompanied by innate immune cells, mostly macrophages. We found that interactions with macrophages of certain polarization may help CTCs to survive. We postulate that mechanical and immunochemical profiling of CTCs and co-purifying immune cells (tumor associated circulating cells; TACCs) provide clues about CTCs aggressiveness and the risk of CR. Our specific aims call for determining the role of (1) epithelial-mesenchymal transition and (2) interactions with circulating macrophages in survival-promoting mechanical fitness of CTCs. Combining the cell culture studies with profiling of CTCs will lead to (3) construction of predictive model for early CR detection. According to the Statement of Work (SOW), our goals for this reporting period (months 25-36) were: (a) finishing of the accrual of required number of patients starting ADT; (b) isolation, enumeration, mechanical and molecular profiling as well as immunochemical characterization of TACCs from these patients’ blood; (c) construction of predictive model for patient stratification and early CR prediction; recapitulation of CTC-macrophage interactions in cell culture model: co-culturing of model “CTCs” (prostate cancer cell lines) with model polarized macrophages; the experiments include mechanical and molecular profiling of control and co-cultured “CTCs”; (d) finishing experiments aimed at recapitulation of EMT and recapitulation of “model CTC” – “model macrophage” interactions in cell culture, complete with biophysical and molecular profiling of model cancer and immune cells. This reporting period supposed to be final for the entire project. The work on *in cellulo* model of CTC adaptations and CTC – macrophage interactions progressed successfully as planned. Unfortunately, the COVID-19 pandemic conditions significantly slowed down accrual of new patients and collection of follow-up blood samples for our study, both in 2020 and in 2021. Therefore, we requested a one-year no-cost extension (NCE) of the award to finish the work. The request was granted, the project is now extended for an additional period of performance and will terminate on August 14, 2022.

2. Keywords

androgen deprivation therapy

atomic force microscopy

castration resistance

castration sensitivity

cell adhesion

cell deformation

cell stiffness

circulating tumor cells

cultured cells

epithelial-mesenchymal transition

gene expression

immune cells

immunostaining

liquid biopsy

macrophage

macrophage polarization

mass cytometry

mechanical phenotype

metastasis

prostate cancer

protein expression

single-cell profiling

3. Accomplishments

3.1 The major goals for the three reporting periods (months 1-36), as stated in the approved SOW, with % of completion

Research-Specific Tasks:

Specific Aim 1: We will determine the role of epithelial to mesenchymal transition in mechanical fitness of CTCs.	Months	Participants	% completion (mo. 25-36)
Major Task 1: Recruit post-castration metastatic PCa patients experiencing biochemical recurrence and starting first line ADT	4-26	Drs. Huang, Liss	79
Major Task 2: Isolate and immunostain TACCs from the samples of blood drawn from the patients right before the start of ADT (70 patients, time t0), enumerate CTCs.	4-28		75
Subtask 1: Perform microfiltration, immunostain the cells. Device for cell isolation: ScreenCell CC ha (ScreenCell)	4-26	Drs. Osmulski, Gaczynska, Chen,	79
Subtask 2: Enumerate the isolated and immunostained CTCs and classify them as EpCAM ⁺ or EMT-CTCs according to surface antigen expression.	4-26	Drs. Gaczynska, Osmulski	70
Major Task 3: Collect multiparameter nanomechanical and morphological data on individual isolated CTCs using PeakForce Quantitative Nanomechanics (PF QNM) AFM imaging.	4-30		79
Subtask 1: Collect the AFM images.	4-26	Drs. Osmulski, Gaczynska	79
Subtask 2: Perform image and data analysis on the collected AFM images.	4-30	Drs. Osmulski, Gaczynska	79
Major Task 4: Perform the gene expression analysis on CTCs.	4-26		100

Major Task 5: Recapitulate EMT in cell culture model	6-24		95
Subtask 1: Culture 22Rv1 and DU145 cells (source: ATCC) according to ATCC recommendations. Induce EMT by treatment with TGF- β . Perform mechanical phenotyping of selected cultured cells.	6-18	Drs. Osmulski, Gaczynska	100
Subtask 2: Perform gene expression analysis of cultured cells that were mechanically phenotyped.	6-18	Dr. Chen	80
Specific Aim 2: We will define the role of CTC-macrophage interactions in mechanical fitness of CTCs.			
Major Task 6: Define the functional composition of macrophage population in TACCs preparations isolated from patients' blood.	1-26		100
Subtask 1: Enumerate and classify non-CTC patient-isolated TACCs according to immunostaining, enumerate CTC-immune cell clusters.	1-24	Drs. Gaczynska, Osmulski	100
Subtask 2: Perform the gene expression analysis on randomly selected cells (up to 30) bearing immune cell markers.	1-32	Dr. Chen	100
Major Task 7: Recapitulate the interactions of model "CTCs" (prostate cancer cell lines) cultured with polarized macrophages.	12-30		100
Subtask 1: Co-culture 22Rv1 and DU145 cells with model macrophages derived from U937 cells (source: ATCC). Determine rates of growth of co-cultured cells, enumerate cell clusters.	12-24	Drs. Gaczynska, Osmulski	100
Subtask 2: Perform mechanical phenotyping of selected cultured cells, free or in clusters.	12-24	Drs. Osmulski, Gaczynska	100
Subtask 3: Perform the gene expression analysis on model CTCs and macrophages.	12-30	Dr. Chen	100
Specific Aim 3. We will construct a model for patients' stratification predicting the risk of castration resistance based on the mechanical fitness of CTCs.			

Major Task 8: Collect mechanical and immunocytochemical properties of TACCs isolated at time t1 (6 months or at failure)	6-30		70
Subtask 1: Perform microfiltration, immunostain the cells, enumerate as for t0.	6-30	Drs. Gaczynska, Osmulski	23
Subtask 2: Perform mechanical profiling of CTCs at time t1, perform image and data analysis on the collected AFM images as for t0.	6-30	Drs. Osmulski, Gaczynska	23
Subtask 3: Compare clinical and biophysical/gene expression data at t1	6-30	Drs. Huang, Liss, Gelfond, Osmulski, Gaczynska	70
Major Task 9: Derive a score for patients' stratification based on the mechanical and immunocytochemical profiling of TACCs	24-36		50
Subtask 1: Develop a mathematical model of EMT and macrophages contribution to the mechanical fitness of CTCs using growth and phenotypic parameters extracted from the cell culture and t0-t1 patients' TACCs data. The model will aid developing the score in Subtask 2.	24-30	Drs. Gelfond, Osmulski	50
Subtask 2: Based on the cumulative mechanical, immunocytochemical and gene expression data construct a risk score for PT stratification and CR prediction.	30-36	Drs. Huang, Gelfond, Liss, Osmulski, Chen, Gaczynska	50

3.2 Specific accomplishments under the Major Tasks listed above:

3.2.1 *Specific Aim 1, Major Task 1*

We planned to accrue a total of 70 metastatic prostate cancer patients starting first-line ADT. During the first 12 months of the project duration we were on-target, with a total of 38 patients (54%) accrued. Unfortunately, the slow-down in accrual caused by the COVID-19 pandemic continued through the third reporting period. As summarized in Table 1, we were able to accrue 9 new patients and collect 10 blood samples from September 2020 to August 2021, and we are still 15-patients short from the target number, with 79% of the accrual completed. The slow-down was a reason of our request for no-cost extension (NCE) of the project. The request was granted.

Table 1 presents the accrual numbers, with information on data collected, relevant for Major Tasks 1-4, 6 and 8, total and specifically in the current reporting period (period 3; 08/15/2020 – 08/14/2021).

Number	Total	This reporting period	Total 1st visit only (t0)	Total two visits (t0 and t1)
Patients (PTs) accrued	55	9	39	16
PT samples with TACCs Collected for Mechanical and Immunochemical Phenotyping	71	10	39	32
TACCs Retained on Filters (approximately)	11000	2000	5800	4700
PT Samples Mechanically Phenotyped	71	10	39	32
PT Samples with Mechanical Phenotype Analyzed	56	10	24	32
CTCs with Mechanical Phenotype Collected	1227	205	676	551
CTCs with Mechanical Phenotype Analyzed	865	186	370	495
PT Samples with Immunostaining Performed and Cell Images Collected	71	10	39	32
Immunostaining Images Collected	2800	395	1521	1279
PT Samples with TACCs Enumeration Completed	46	17	22	24
PT Samples with Cells Collected for Gene and Protein Expression Analysis	71	10	39	32
PT Samples with TACCs analyzed by single-cell transcriptomics	20	0	20	0
CTCs analyzed by single-cell transcriptomics	273	0	273	0
Immune cells analyzed by single-cell transcriptomics	143	0	143	0

3.2.2 Specific Aim 1, Major Task 2

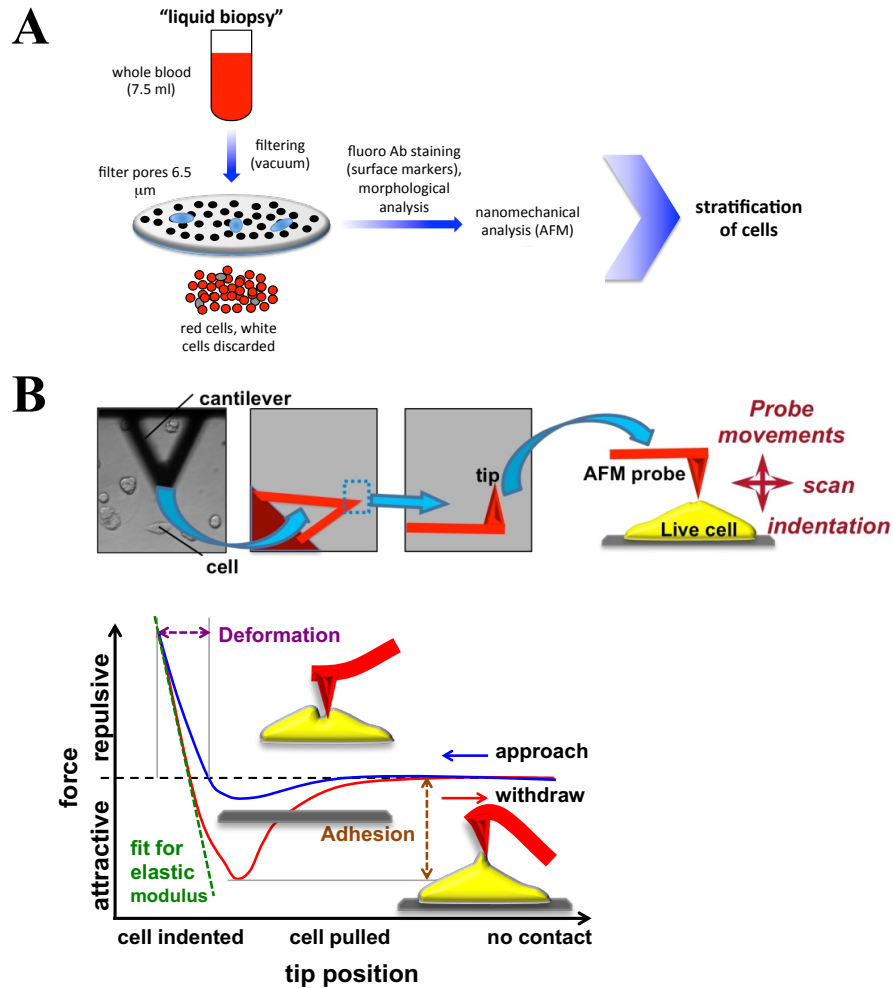


Figure 1 Processing of liquid biopsy samples from prostate cancer patients (as in report period 1).

A: isolation of large tumor associated circulating cells (TACCs). A separate filter is used to collect additional TACCs for gene and protein expression analysis. **B:** nanomechanical profiling: a small silicon probe on a cantilever “pokes” the cell with extremely small (nanoNewton-scale) force to collect “force curves” used to extract precise numerical data on elasticity (reversible change of shape), deformability (reversible and non-reversible, nondestructive change of shape) and adhesiveness.

As in previous reporting periods for all blood samples we collected filters with retained cells and images of immunostained TACCs (*Subtask 1*). The patient’s blood samples were processed within two hours from phlebotomy, as planned. Processing included microfiltration with the ScreenCell device retaining all cells that do not pass through 6.5 μm pores randomly distributed in the filters. The filters are formulated for cells’ adherence, important to hold cells for AFM profiling. The cells still attached to the filters are subjected to nanomechanical imaging. The methods of processing

and AFM imaging did not change since the last reporting period and are presented above in **Figure 1**.

All large cells collected on filters are immunostained and photographed for enumeration and classification. To date, we fully enumerated and classified CTCs for more than half of collected samples (*Subtask 2*). See **Table 1** for details. Analysis of correlations of enumeration of distinct classes of CTCs and mechanical phenotypes of CTCs is presented below, with a progress report for *Specific Aim 1, Major Task 3*.

3.2.3 *Specific Aim 1, Major Task 3*

Mechanical phenotypes of single CTCs were collected with atomic force microscopy (AFM) PeakForce Quantitative Nanomechanical mode for all collected samples immediately after microfiltration, as planned (*Subtask 1*). As for now, the collected data are fully processed and analyzed for a total of 56 samples (*Subtask 2*; see **Table 1** for details). For all analyzed CTCs, a full mechanical phenotype with cell elasticity, deformation and adhesion, was collected.

With the mechanical and immunochemical phenotypes analyzed for a significant number of patient samples, we attempted to classify the expectedly diverse cells from a subset of 23 patients (*Subtask 2*). The classification of 514 CTCs isolated from 33 samples including both t0 and t1 visits was presented in the 2020 report, and resulted in distinguishing of four categories of CTCs based on their mechanical phenotypes. The updated classification was the core of paper published in August 1 issue of *Cancer Research*, and highlighted in the journal's issue, with AFM-derived images of scanned CTCs and accompanying immune cells on the *Cancer Research* cover (**Figure 2**).



Highlight:

Contacts with Macrophages Promote an Aggressive Nanomechanical Phenotype of Circulating Tumor Cells in Prostate Cancer

Pawel A. Osmulski, Alessandra Cunsolo, Meizhen Chen, Yusheng Qian, Chun-Lin Lin, Chia-Nung Hung, Devalingam Mahalingam, Nameer B. Kirma, Chun-Liang Chen, Josephine A. Taverna, Michael A. Liss, Ian M. Thompson, Tim H.-M. Huang and Maria E. Gaczynska DOI: 10.1158/0008-5472.CAN-20-3595 Published August 2021

About the cover: Circulating tumor cells (CTC) and macrophages interact and form pairs. The interactions increase metastatic potential of CTCs. Atomic force microscopy (AFM) imaging created the pseudo-3D reliefs of CTCs (yellow-orange-red) and macrophages (blue-navy-green), isolated from the blood of prostate cancer patients. Nanomechanical analysis by AFM helped to assess mechanical fitness of CTCs, indicating their capacity to survive and initiate metastasis.

Figure 2 The research performed as a part of this project was described in the recent *Cancer Research* paper and was highlighted in the journal's August 1, 2021 issue. The paper introduced the concept of “mechanical fitness” of CTCs (*Specific Aim 1, Major Task 3*), presented how the fitness is associated with EMT plasticity (*Specific Aim 1, Major Tasks 2 and 5*) and with the presence of circulating macrophages co-purifying with CTCs (see below *Specific Aim 2, Major Tasks 6 and 7*).

Figure 3 presents the updated classification of CTCs into the categories, and updated “mechanical fitness chart” based on the classification. CTCs in categories 3 and 4 were exceptionally soft and exceptionally adhesive, respectively, and considered “best fit” to survive and thrive in circulation.

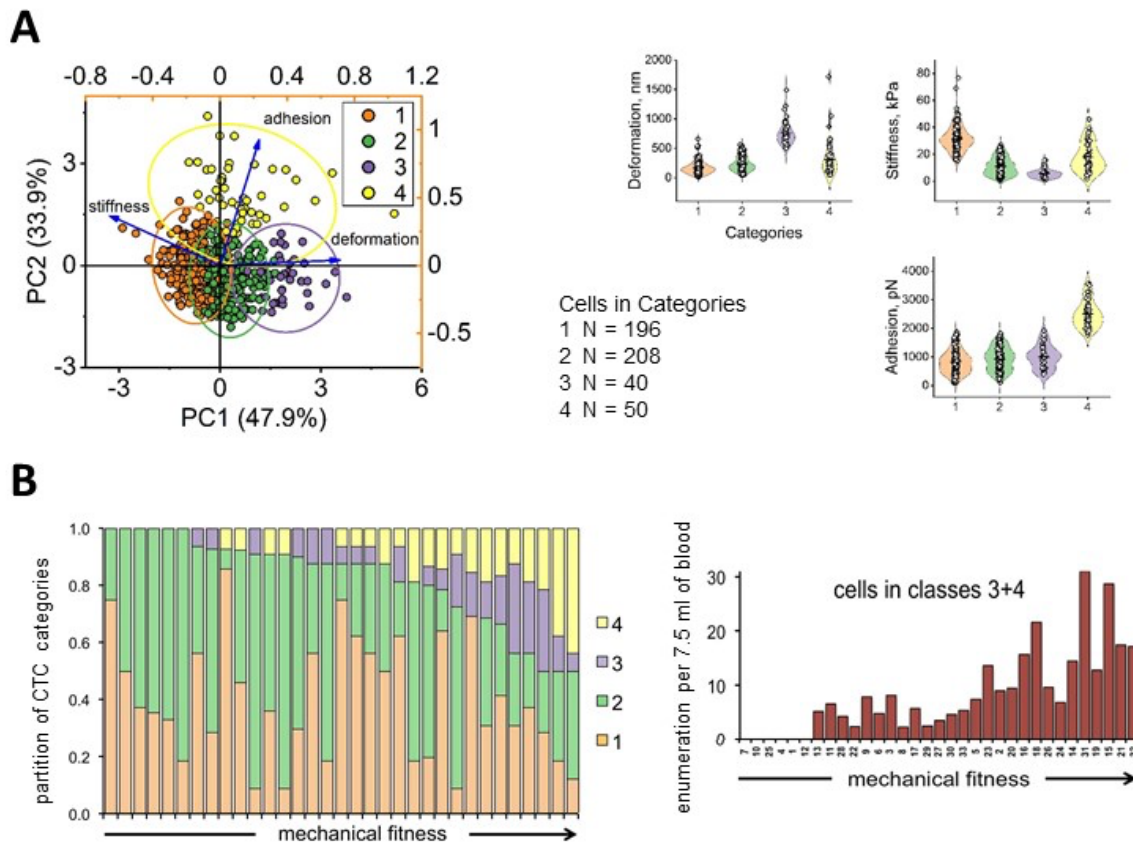


Figure 3 (updated from Figures 3 and 4 from the previous report) **Phenotypic diversity and mechanical fitness of 494 CTCs isolated from 33 blood samples from 23 patients.** **A.** Principal component analysis (PCA; left) reveals the presence of four categories of cells with distinct mechanical phenotypes (right). Cell categories were identified with the unsupervised hierarchical clustering. Categories 3 and 4 contain the softest and most adhesive cells, respectively, that we consider the most “mechanically fit” to withstand mechanical stress in the bloodstream, survive and proceed with extravasation and seeding metastasis. **B.** The “CTC fitness chart” of prostate cancer patients. Each column represents data for CTCs isolated from a single blood sample. The samples are ordered according to relative abundance of CTCs belonging to best-fit mechanical categories 4 and 3. Right: enumeration of cells in categories 3 and 4 followed the “fitness axis” of relative abundance of CTCs.

The uniqueness of mechanical fitness as a special feature of CTCs and not tumor cells in general was demonstrated by comparison of mechanical phenotypes of CTCs and “urine prostate cells” (UPCs) shed by prostate tumors to the urine of patients. Both CTCs and UPCs are exposed to damaging fluid shear stress; however only CTCs may act as “seeds of metastasis” while UPCs inevitably perish. We used nanomechanical parameters collected for 122 CTCs (n=10 patients) and 104 UPCs (n=11 patients) positive for prostate-specific markers PSA/PSMA. The patient cohort was comprised of high-risk patients with local disease and patients with low-volume metastatic spread. The data for UPCs were collected in the past, whereas CTCs were collected from the blood of patients (a random subset) accrued for this study. The striking difference between mechanical phenotypes of CTCs and UPCs is apparent in **Figure 4**. With principal component analysis (PCA), we found that CTCs appeared five-fold more adhesive than UPCs. Analysis of stiffness and deformability revealed a remarkable diversity among UPCs: one class of UPCs was not significantly different from CTCs, whereas the other class was almost seven times stiffer than CTCs (**Figure 4**). We speculate that those stiff UPCs may undergo apoptosis, consistently with published data reporting cell death accompanying increase in stiffness. High softness and low adhesion are known mesenchymal hallmarks of aggressive cancer cells, and the soft, non-adhesive class of UPCs embodied these traits. However, the majority of CTCs retained epithelial adhesion. At the same time the CTCs displayed mesenchymal properties for softness. Consistently, we recognized high adhesion and softness as distinctive “mechanical fitness” features demonstrated by CTCs but not by UPCs. Since CTCs may originate from metastatic sites, not only the primary tumor as assumed for UPCs, we tested if CTCs isolated from patients with confirmed distant spread at the time of blood draw would form a separate class. Two out of ten patients used for this study were metastatic, however phenotypes of their CTCs did not form a separate class in the population of all CTCs (**Figure 4** – right). This outcome points out that CTCs are not only detectable in blood, but also can be distinctively aggressive even before distant spread is clinically confirmed.

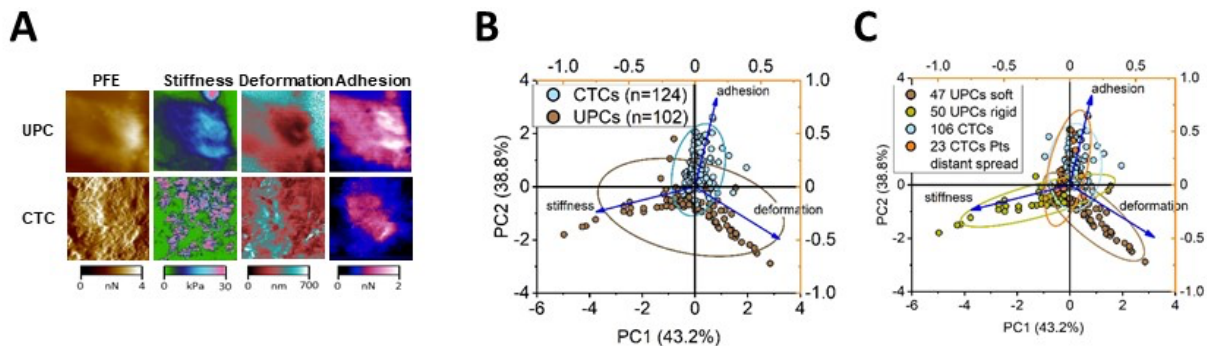


Figure 4 Urine prostate cells (UPCs) and circulating tumor cells (CTCs) present distinct nanomechanical properties. **A.** Comparison of typical examples of mechanical properties between a UPC and CTC. Each row represents the same single cell and its mechanical properties are arranged in columns. The first column: cell topography (peak force error channel; PFE; Bruker). In this example the UPC was more stiff, less deformable and more adhesive than the CTC. Images were false colored using scales covering the data extension; scale 10x10µm. **B and C:** Principal component analysis (PCA) based on the mechanical phenotype of cells separates population of 122 CTCs (n=10 patients) from 104 UPCs (n=11 patients), with CTCs generally more adhesive than UPCs. **C.** CTCs isolated from metastatic patients are colored differently than CTCs from high-risk patients with no distant spread detected at the time of blood draw.

3.2.4 Specific Aim 1, Major Task 4

The CTCs were collected (*Subtask 1*) and the gene expression analysis was performed for a subset of collected CTCs (*Subtask 2*), as planned. The *Task 4* was 100% completed in the previous reporting period, and the data were presented in the 2020 report.

3.2.5 Specific Aim 1, Major Task 5

The *Subtask 1*: culturing 22Rv1 and DU145 cells, inducing EMT by treatment with TGF- β or EMT-inducing media supplement and performing mechanical phenotyping of selected cultured cells, was completed in the previous reporting period, as planned. The data were presented in the 2020 report and included discussion on the EMT plasticity in CTCs and cultured cells model.

The *Subtask 2* (gene expression analysis) is nearing completion. The proteomic analysis of the cells with mass cytometry (CyTOF) is advancing and will be finished shortly. It was planned to be completed by now, however unexpected periodic shortages of specialized laboratory supplies and reagents delayed the task. While waiting to accommodate the shortages, we performed a set of pilot experiments on cultured prostate cancer cells exposed to fluid shear stress (FSS) mimicking the conditions experienced by the CTCs in circulation. We used microfluidic system (IBIDI) that generates highly controlled conditions mimicking fluid flow in veins, arteries or capillaries. We hypothesized that FSS may induce EMT-related changes in the “model tumor cells”, thus transforming them into “model CTCs”. The pilot data were consistent with our hypothesis. As demonstrated in **Figure 5A**, mesenchymal markers vimentin and N-cadherin were up-regulated in DU145 cells even after a short exposure to FSS. To the contrary, cytokeratins (epithelial markers; cytokeratin 19 and cytokeratin 8/18) were down-regulated under the same conditions, as compared to non-stressed DU145 cells. Importantly, nanomechanical profiling of these cells presented in **Figure 5B** revealed FSS-induced increase in cell adhesiveness (non-EMT trait) and increased softness (EMT trait), pointing at epithelial-mesenchymal plasticity (hybrid EMT) of “model CTCs” and their improved mechanical fitness. These observations constitute an excellent starting point for future follow-up studies to reveal mechanisms of CTCs adaptation to circulation stress.

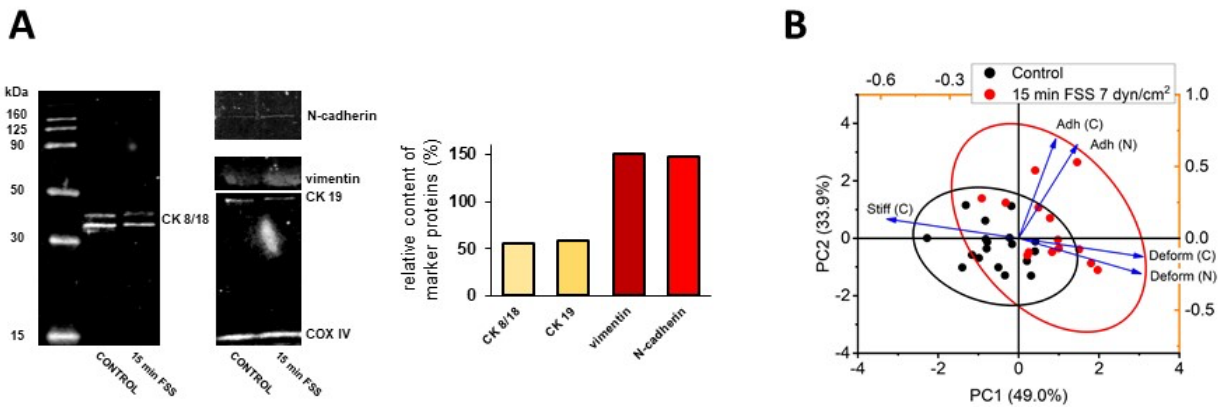


Figure 5 Short-time fluid shear stress (FSS) challenge induces hybrid EMT and improves mechanical fitness of DU145 cells. We tested a 15 min challenge under conditions imitating blood flow in small veins or large capillaries. The viability of cells remained at 90% for control (floating, not stressed cells) and stressed cultures. **A.** Proteins from lysates prepared from control and stressed cells were separated by SDS-PAGE (denaturing polyacrylamide gel electrophoresis), transferred to nitrocellulose membrane (Western blotting) and probed with specific antibodies recognizing mesenchymal and epithelial marker proteins, and COX IV (cytochrome c oxidase subunit 4; a loading control). Protein bands were visualized with Odyssey Infrared Imaging System (Li-Cor). Relative contents of protein markers are presented (control circulated without FSS: 100%), adjusted for loading (COX IV used as loading control). **B.** PCA of mechanical parameters (*right*; each dot represents a unique cell) revealed that cells responded to the short stress with an increased adhesion and softness, indicating improved mechanical fitness. “C” and “N” designate mechanical parameters measured above cytoplasm or above nuclear region of the cell, respectively.

3.2.6 Specific Aim 2, Major Task 6

The immunostaining-based composition of non-CTC, immune cells population in TACCs (*Subtask 1*) was determined for additional patient-isolated samples, as stated in **Table 1**. Data for the *Subtask 2*, a gene expression analysis on a sample of immune cells, were presented in the 2020 reporting period. The *Task 6* is now completed. Immune cells will be immunostained and enumerated in the samples of patients yet-to-be accrued as a part of *Specific Aim 3*.

The data collected and analyzed for the *Task* were included in the published *Cancer Research* paper. A presumed unique relationship between CTCs and co-isolating immune cells was further demonstrated by our comparison between populations of tumor cells shed to urine (see above on *Major Task 3*) and shed to blood (tumor-associated circulating cells; TACCs). Both blood retentates and urine sediments contained EpCAM⁺ cells but also numerous EpCAM⁻ cells positive for pan-leukocyte marker CD45 (leukocyte common antigen; **Figure 6A**). Morphometric analysis of a random sample of light/fluorescent microscopy images of these cells revealed that EpCAM⁺ cells were predictably large in both blood and urine preparations. Footprints of these cells corresponded to squares with average lengths of 24 μm (44 CTCs; range of lengths 10 μm – 32 μm) or 21 μm (51 UPCs; range of lengths 8 μm – 30 μm), well within morphological parameters reported for CTCs. Population of CTCs with larger footprints was more numerous than a similar population in UPCs (**Figure 6B**). This may reflect the high content of CTC pairs in blood retentates (cells retained on the filter; **Figure 1**), consistent with high adhesiveness of CTCs as compared to UPCs. Such cell pairs are customarily counted as single objects in FDA-approved diagnostic/prognostic enumerations of CTCs. In turn, footprints of the immune cells found in urine sediments were rather small (average diameter 10 μm , range 6 μm – 18 μm ; **Figure 6B**) corresponding to typical leukocytes with expected diameters ranging from 7 μm to 15 μm . Instead, blood-derived EpCAM⁻CD45⁺ cells had an average diameter of 23 μm , (range: 16 μm – 25 μm ; **Figure 6B**). The observed difference in size distribution could not be attributed solely to the

expected enrichment of blood retentates in large cells, as partitions of tumor-to-immune cells were very similar, close to 1:1, in preparations recovered from the two types of liquid biopsies (see caption to **Figure 6**). However, large immune cells were absent in urine. Those large cells are macrophages.

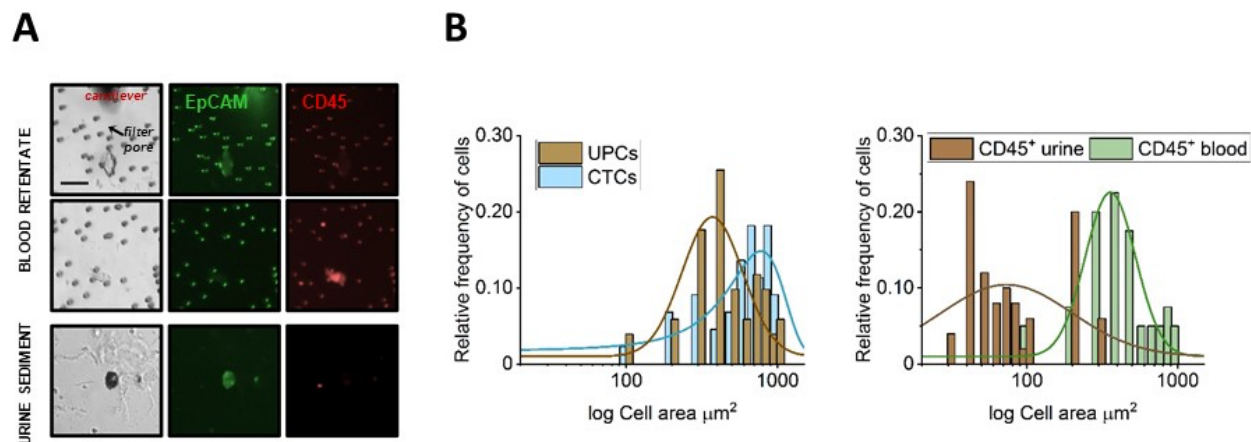


Figure 6 Tumor cells and immune cells are isolated from urine and blood liquid biopsies collected from patients with aggressive prostate cancer, however large immune cells are present only in blood. **A.** Cells from blood (two top rows) were isolated by microfiltration, cells from urine were sedimented; next they were stained with anti-EpCAM and anti-CD45 (pan-leukocyte) fluorescently labelled antibodies. The filter pores and the AFM cantilever may reflect glow from the labels as an artifact. **B.** Morphometric analysis of footprints (area) of: Left - CTCs and UPCs (EpCAM⁺CD45⁻; 44 and 40 cells, respectively; $p < 0.0002$ Kolmogorov-Smirnov test) and Right – EpCAM⁻CD45⁺ cells captured in blood filtrates (51 cells) and in urine sediments (50 cells) of 21 prostate cancer patients; $p < 0.0001$ Kolmogorov-Smirnov.

3.2.7 Specific Aim 2, Major Task 7

Recapitulation of the interactions between model CTCs (prostate cancer cell lines) and model macrophages was completed ahead of schedule in the 2020 reporting period (all three *Subtasks*). The data were presented in the 2020 report and are included in the *Cancer Research* paper.

3.2.8 Specific Aim 3, Major Task 8

To date, samples were collected for 16 patients with both t0 and t1 visits (**Table 1**). While collection of t0 samples is delayed by the COVID-19 pandemic, but nevertheless nearly 80% completed, the collection of t1 samples is severely affected. Fortunately, clinical status: sensitivity or resistance to ADT, of all accrued patients, was recognized even when t1 blood samples for TACCs analysis were not collected. Therefore, we continue to work on the *Task* with available

data, both nanomechanical and immunocytochemical profiles (*Subtasks 1 and 2*) and with clinical updates (*Subtask 3*), and we consider the task to be highly advanced, progressing with collection and analysis of t0 samples and with clinical updates.

Highly encouraging results of test cluster analysis on the biophysical data were presented in the 2020 report and are included in the *Cancer Research* paper. The analysis revealed that patients that remained CS for up to a year after t0 tended to cluster together. Also, our presented before cluster analysis of mechanical and enumeration parameters separated cases according to a metastatic spread status. With more patient data available we refined our analysis (*Subtask 3*).

As presented in **Figure 7**, we analyzed cells isolated from the blood of 28 high risk/low-volume metastatic castration sensitive prostate cancer patients starting or undergoing androgen deprivation therapy (ADT). Hierarchical Cluster Analysis of mechanical and immunocytochemical parameters identified three groups of patients. Clinical updates collected after the analysis indicated that the risk of developing castration resistance (CR) within 4-20 months from t0 sampling differed greatly between the groups. In one group (“green”) all patients remained CS for at least 34-45 months (no CR). The other two groups (“navy” and “red”) show a low and high CR development risk within 4-20 months from sampling (two-sample proportion test: exact $p=0.249$). Unexpectedly, enumeration of EpCAM⁺ “canonical” CTCs was associated with long term CS, in contrast to enumeration of CTC-EMT and certain classes of MΦs. This underlines the shortcoming of EpCAM-based methods of CTC isolation, including the sole FDA-approved method, that neglect EpCAM-negative CTCs and accompanying immune cells. Although the risk prediction did not reach statistical significance, power analysis indicates that it can be prudently tested with the number of patients that we intend to accrue and analyze.

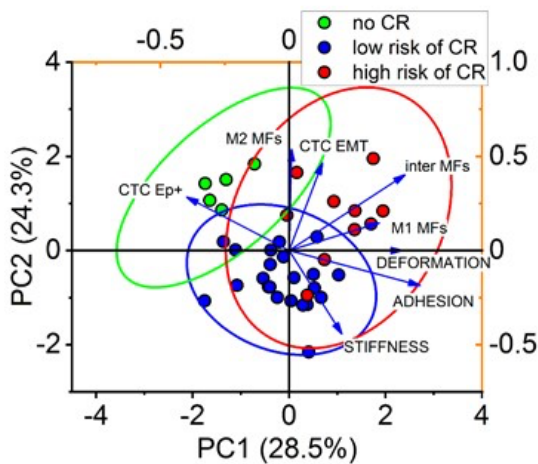


Figure 7 Predictive potential of nanomechanical phenotyping combined with immunocytochemical analysis of TACCs. Principal component analysis (PCA) of adhesion, deformation and stiffness of CTCs, as well as enumeration of EpCAM⁺ CTCs, EMT-undergoing EpCAM⁻ CTCs and three classes of macrophages, is shown at *right*; each dot represents data of a single patient.

The most unexpected finding of our research to-date was that enumeration of M1-like CD80⁺ CD163⁻ macrophages associated with a high mechanical fitness of CTCs (reported in 2020 and in *Cancer Research* paper) and with a high risk of CR (**Figure 7**). Our starting hypothesis was that pro-inflammatory M1-like macrophages would act as “predators” attacking CTCs, in contrast to M2-like anti-inflammatory protective “chaperones” of CTCs. One explanation, discussed in the *Cancer Research* paper, is that macrophages co-purifying with CTCs, including M1-like macrophages, are derived from diverse and pro-cancer tumor-associated macrophages (TAMs). In fact, the CD80⁺ CD163⁺ macrophages are frequent among TAMs and we detect them in great numbers among TACCs. We envision that CTCs leaving the tumor are taking a “mini-tumor microenvironment”, most notably TAMs, with them. Another possibility worth considering is that M1-like macrophages are recruited from the blood, however fail to destroy CTCs and are ultimately “hijacked” by CTCs as chaperones. Our co-culture experiments with model tumor cells and model M1-type or M2-type macrophages conformed that macrophages of both polarizations are capable of supporting mechanical fitness of tumor cells (*Major Task 7*). To learn more about the potential CTC-macrophages associations, we attempted to mathematically model the dynamic interactions between these cells. As demonstrated in **Figure 8**, even if M1-like macrophages are “predators” for CTCs, the former may never exterminate the latter, ultimately allowing for metastasis. Moreover, M1-like macrophages may be recruited by CTCs to support their survival (**Figure 8 - rightmost**).

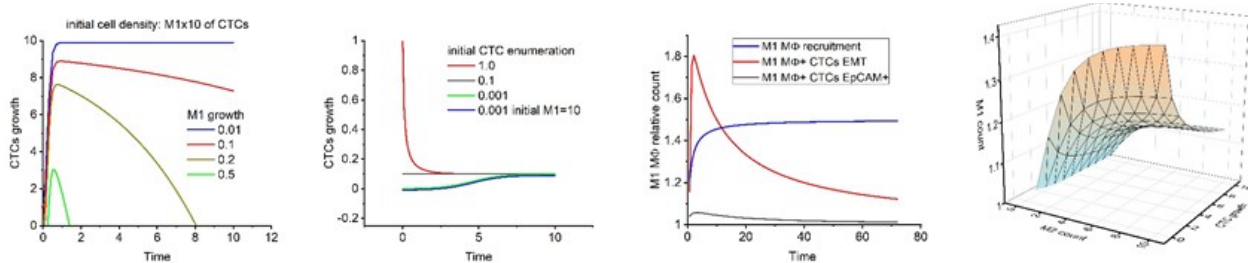


Figure 8 Assessing dynamics of nanomechanical phenotypes of model prostate cancer cells co-cultured with model macrophages. Gompertz model of cell cancer growth modified by the presence of M1 (anti-tumor) and M2 (pro tumor) macrophages. From left to right: content of CTCs constant, content of M1 constant, model with recruitment of macrophages by CTCs, model of cells’ growth with CTCs, M1, and M2 macrophages present.

3.3 Opportunities for training and professional development provided by the project:

- Dr. Chia-Nung Hung, Postdoctoral Fellow, contributed mass cytometry proteomic profiling of cells for the project. He mastered the method and is a co-author of the *Cancer Research* paper.
- Yusheng Qian, M.Sc., a senior PhD Graduate Student in Molecular Medicine is continuing his work on the project. He is a co-author of the *Cancer Research* paper. He generated data for *Major Tasks 5 and 7*, and the project will constitute a core of his PhD thesis. He is extending the work into a unique AFM-based characterization of single cell-to-cell

interactions. He presented the work in virtual meetings and is currently finishing preparation of a first-author manuscript describing the use of the method for model CTCs.

3.4 Dissemination of the results to communities of interest:

Poster presentations (presenter underlined):

Pawel A. Osmulski, Alessandra Cunsolo, Yusheng Qian, Meizhen Chen, Chun-Lin Lin, Chia-Nung Hung, Devalingam Mahalingam, Nameer Kirma, Chun-Liang Chen, Josephine Taverna, Michael Liss, Ian M. Thompson, Tim H.-. Huang, Maria Gaczynska (February 2021) Macrophages support the aggressive mechanical phenotype of circulating tumor cells in prostate cancer.
65th Annual Biophysical Society Meeting, Biophysical Society, virtual.

Short – talk/poster presentation (presenter underlined):

Pawel A. Osmulski, Alessandra Cunsolo, Yusheng Qian, Meizhen Chen, Chun-Lin Lin, Chia-Nung Hung, Devalingam Mahalingam, Nameer Kirma, Chun-Liang Chen, Josephine Taverna, Michael Liss, Ian M. Thompson, Tim H.-. Huang, Maria Gaczynska (May 2021) Aggressive mechanical phenotype of circulating tumor cells in prostate cancer is supported by contacts with macrophages. The Robert A. Clark Frontiers of Translational Science Research Day (San Antonio, TX)

Yusheng Qian, Alessandra Cunsolo, Meizhen Chen, Chia-Nung Hung, Nameer B. Kirma, Michael Liss, Tim H. Huang, Pawel A. Osmulski, Maria E. Gaczynska (February 2021) Strategies of mechanical adaptation of CTCs to blood circulation.
65th Annual Biophysical Society Meeting, Biophysical Society, virtual.

COMMENT: As in previous reporting period there was no traditional in-person meetings. Instead, we presented the work on available virtual meetings.

3.5 Plans for the next reporting period:

In the no-cost extension period we will continue the study following the Statement of Work for months 24-36.

- A final cohort of patients should be accrued.
- Mechanical and immunochemical profiles will be collected for all accrued patients.
- All collected biophysical and molecular data will be analyzed.
- Statistical analysis of mechanical, immunochemical, molecular and clinical data will be performed.
- The patient-derived and cell model data will be integrated into a model of CTCs behavior, focused on epithelial-mesenchymal plasticity and macrophages' contribution.
- A score for patients' risk stratification and CR prediction will be constructed.

4. Impact

4.1 Impact on the development of the principal discipline of the project.

The major findings in this reporting period are outlined below.

- We confirmed and refined our initial finding that patient isolated CTCs and model prostate cancer cells display unique epithelial-mesenchymal plasticity, with high adhesiveness (epithelial trait) confirmed as the major nanomechanical parameter distinguishing aggressive tumor cells from aggressive CTCs. We propose that invasive tumor-residing cells already advanced on the EMT axis may reverse to regain high adhesion, useful for survival-promoting clustering in circulation. At the same time, we observe that CTCs of patients with rapid metastatic spread are poorly adhesive, most likely indicating their regained EMT advance and high invasiveness.

Significance: the finding broadens the knowledge about the diversity of cancer-related epithelial-to-mesenchymal transition. The concept of epithelial-mesenchymal plasticity is now gaining increased interest as critical for understanding cancer cells transition to invasiveness. Importantly, the knowledge will impact development of anti-metastasis therapies, with targeting adhesiveness of CTCs as an attractive goal not explored before.

- We confirmed association of mechanical fitness of patient-isolated CTCs with abundance of macrophages with markers of TAMs. We speculate that macrophages that co-purify with CTCs are in fact TAMs that escaped the tumor, possibly in clusters with CTC. Importantly, abundance macrophages with M1-like features and mixed M1/M2 phenotypes is especially strongly associated with high mechanical fitness and poor prognosis. We hypothesize that the M1-like macrophages could be recruited from diverse TAM population or from the blood monocytes. We will explore the notions.

Significance: Enumeration of macrophages emerges as a predictive marker, alone or together with mechanical phenotype and enumeration of CTCs. Targeting macrophages emerges as a viable anti-metastatic strategy. The findings also point at diversity of TAMs and at critical involvement of immune cells in metastasis.

4.2 Impact on other disciplines.

Nothing to Report

4.3 Impact on technology transfer.

Nothing to Report

4.3 Impact on society beyond science and technology.

Nothing to Report

5. Changes/problems

5.1 Changes in approach and reasons for change.

There are no significant changes in approach. Minor changes and additions:

- With limited supply of t1 blood samples we rely more on available clinical updates for the accrued patients. The extensive updates are sufficient to construct our predictive score as declared in SOW.

5.2 Actual or anticipated problems or delays.

The project will be in NCE for the next year. The delay is caused by COVID-19 pandemic related slowdown in patients' accrual. The tasks not related to patients accrual are either finished or near completion.

5.3 Changes that had a significant impact on expenditures.

None

5.4 Significant changes in use or care of human subjects/vertebrate animals/biohazards/select agents.

None

6. Products

- Paper published (highlighted with a cover):

Osmulski PA, Cunsolo A, Chen M, Qian Y, Lin CL, Hung CN, Mahalingam D, Kirma NB, Chen CL, Taverna JA, Liss MA, Thompson IM, Huang TH, Gaczynska ME. (2021) Contacts with Macrophages Promote an Aggressive Nanomechanical Phenotype of Circulating Tumor Cells in Prostate Cancer. *Cancer Res.* 2021 Aug 1;81(15):4110-4123. doi: 10.1158/0008-5472.CAN-20-3595. PMID: 34045187.

7. Participants

7.1 Individuals working on the project

Name	Tim H. Huang
Project Role	PI
Researcher Identifier (e.g. ORCID ID):	0000-0001-5985-9176
Nearest person month worked:	0.96 cal. mo.
Contribution to Project:	Oversight and coordination of the project
Funding Support:	No Change

Name	Maria Gaczynska
Project Role	Co-Investigator
Researcher Identifier (e.g. ORCID ID):	0000-0002-9033-5706
Nearest person month worked:	3 cal. mo.
Contribution to Project:	Collection and analysis of immunofluorescence images of TACCs, design and oversight of co-culture experiments.
Funding Support:	No Change

Name	Pawel A.Osmulski
Project Role	Co-Investigator
Researcher Identifier (e.g. ORCID ID):	0000-0002-5359-9200
Nearest person month worked:	1.8 cal. mo.
Contribution to Project:	Collection and analysis of mechanical phenotypes of patient isolated and model CTCs, design of co-culture experiments.
Funding Support:	No Change

Name	Chun-Liang Chen
Project Role	Co-Investigator
Researcher Identifier (e.g. ORCID ID):	0000-0002-6774-9003
Nearest person month worked:	1.2 cal. mo.
Contribution to Project:	Collection of cells for single-cell gene expression analysis, single cell gene expression analysis of selected CTCs.
Funding Support:	No Change

Name	Michael Liss
Project Role	Co-Investigator
Researcher Identifier (e.g. ORCID ID):	0000-0001-6978-1026
Nearest person month worked:	.36 cal. mo.

Contribution to Project:	Coordination of patients' accrual, collection of clinical data.
Funding Support:	No Change

Name	Byeongyeob Choi
Project Role	Co-Investigator
Researcher Identifier (e.g. ORCID ID):	
Nearest person month worked:	.6 cal. mo.
Contribution to Project:	Processing of data for statistical analysis
Funding Support:	No Change

Name	Meizhen Chen
Project Role	Research Scientist
Researcher Identifier (e.g. ORCID ID):	
Nearest person month worked:	.6 cal. mo.
Contribution to Project:	Co-culture experiments with model CTCs and macrophages.
Funding Support:	No Change

Name	Chia-Nung Hung
Project Role	Research Scientist
Researcher Identifier (e.g. ORCID ID):	
Nearest person month worked:	3 cal. mo.
Contribution to Project:	CytoF analysis of model CTCs and macrophages, collection of cells for single-cell gene expression analysis, single cell gene expression analysis of selected CTCs, model CTCs and model macrophages.
Funding Support:	No Change

Name	Yusheng Qian
Project Role	Graduate Student
Researcher Identifier (e.g. ORCID ID):	
Nearest person month worked:	6 cal. mo.
Contribution to Project:	Co-culture experiments with model CTCs and macrophages, collection and analysis of mechanical phenotypes of model CTCs.
Funding Support:	No Change

7.2 Changes in the active other support of PD/PI and key personnel

Nothing to report

7.3 Other organizations involved as partners

Nothing to report

8. Special Reporting Requirements

Nothing to report

9. Appendices

Contacts with Macrophages Promote an Aggressive Nanomechanical Phenotype of Circulating Tumor Cells in Prostate Cancer



Pawel A. Osmulski¹, Alessandra Cunsolo¹, Meizhen Chen¹, Yusheng Qian¹, Chun-Lin Lin¹, Chia-Nung Hung¹, Devalingam Mahalingam², Nameer B. Kirma¹, Chun-Liang Chen¹, Josephine A. Taverna², Michael A. Liss³, Ian M. Thompson³, Tim H.-M. Huang¹, and Maria E. Gaczynska¹

ABSTRACT

Aggressive tumors of epithelial origin shed cells that intravasate and become circulating tumor cells (CTC). The CTCs that are able to survive the stresses encountered in the bloodstream can then seed metastases. We demonstrated previously that CTCs isolated from the blood of prostate cancer patients display specific nanomechanical phenotypes characteristic of cell endurance and invasiveness and patient sensitivity to androgen deprivation therapy. Here we report that patient-isolated CTCs are nanomechanically distinct from cells randomly shed from the tumor, with high adhesion as the most distinguishing biophysical marker. CTCs uniquely coisolated with macrophage-like cells bearing the markers of tumor-associated macrophages (TAM). The presence of these immune cells was indicative of a survival-promoting phenotype of “mechanical fitness” in CTCs based on high softness and high adhesion as determined by atomic force microscopy. Correlations between enumeration of macrophages and mechanical fitness of CTCs were

strong in patients before the start of hormonal therapy. Single-cell proteomic analysis and nanomechanical phenotyping of tumor cell–macrophage cocultures revealed that macrophages promoted epithelial–mesenchymal plasticity in prostate cancer cells, manifesting in their mechanical fitness. The resulting softness and adhesiveness of the mechanically fit CTCs confer resistance to shear stress and enable protective cell clustering. These findings suggest that selected tumor cells are coached by TAMs and accompanied by them to acquire intermediate epithelial/mesenchymal status, thereby facilitating survival during the critical early stage leading to metastasis.

Significance: The interaction between macrophages and circulating tumor cells increases the capacity of tumor cells to initiate metastasis and may constitute a new set of blood-based targets for pharmacologic intervention.

Introduction

Circulating tumor cells (CTC) are shed by aggressive epithelial-origin tumors and are found in the bloodstream of patients at the risk of metastasis or with already detected metastatic growth (1). CTCs are as rare as one in a billion of blood cells, however, due to their unique large size and epithelial surface markers, they can be isolated by microfiltration or immunoaffinity capture from a “liquid biopsy”—few milliliters of a patient’s peripheral blood (1, 2). Because the

bloodstream is not a natural environment for epithelial-like CTCs, majority of them die by mechanical stress, apoptosis or anoikis, or removed by immune cells (3, 4). The surviving few CTCs progress with epithelial-to-mesenchymal transition (EMT), extravasate, and start new tumor growth (1, 3). Enumeration of CTCs is used as a general prognostic biomarker (2). However, the enumeration-only approach centered on EpCAM (epithelial cell adhesion molecule) positive cells neglects heterogeneity of CTCs (5). Because successful CTCs need a specific sequence of adaptations to withstand mechanical challenges during intravasation, circulation, and extravasation, we turned our attention to their physical endurance (6). These physical properties are tightly connected to EMT-related massive remodeling of the cytoskeleton and membranes affecting cell softness and adhesion (5). EMT traits are considered biomarkers of poor prognosis (7). However, CTCs express a wide spectrum of both epithelial and mesenchymal marker proteins, a hallmark of not fully understood epithelial–mesenchymal plasticity (EMP; ref. 5). Indeed, recent evidence suggests that the ability to adopt and traverse intermediate epithelial/mesenchymal (E/M) states, is a crucial adaptive strategy for CTCs (5).

In our previous works, we have demonstrated that CTCs isolated from the blood of castration resistant patients are significantly less stiff, more deformable and more adhesive than CTCs from castration sensitive patients with less aggressive disease responding to androgen deprivation therapy (ADT; ref. 8). Because castration resistant patients are at high risk of fast metastatic spread, we proposed that CTCs isolated from these patients are “mechanically fit”: well adapted to escape death in circulation and to invade distant tissues. Mechanical fitness amounts to a particular nanomechanical phenotype characterized by low stiffness, high deformability and high adhesion. We envision that such CTCs are particularly aggressive, specifically

¹Department of Molecular Medicine, University of Texas Health Science Center at San Antonio, San Antonio, Texas. ²Department of Hematology and Oncology, University of Texas Health Science Center at San Antonio/Mays Cancer Center, San Antonio, Texas. ³Department of Urology, University of Texas Health Science Center/Mays Cancer Center, San Antonio, Texas.

Note: Supplementary data for this article are available at Cancer Research Online (<http://cancerres.aacrjournals.org/>).

Current address for A. Cunsolo: Epic Sciences Inc., San Diego, California; current address for Chun-Lin Lin, Fractal Analytics, New York, New York; current address for D. Mahalingam, Robert H Lurie Medical Research Center, Northwestern University, Feinberg School of Medicine, Chicago, Illinois; and current address for I.M. Thompson, CHRISTUS Santa Rosa Hospital - Medical Center, San Antonio, Texas.

Corresponding Authors: Maria E. Gaczynska, University of Texas Health at San Antonio, South Texas Research Facility, 8403 Floyd Curl Drive, San Antonio, TX 78229. Phone: 210-567-7262; E-mail: Gaczynska@uthscsa.edu; and Pawel A. Osmulski, Osmulski@uthscsa.edu

Cancer Res 2021;81:4110–23

doi: 10.1158/0008-5472.CAN-20-3595

©2021 American Association for Cancer Research

Macrophages Promote Aggressive Mechanical Phenotype of CTCs

supporting distant metastases. Importantly, we found that the “low stiffness–high deformability–high adhesion” pattern of mechanical properties distinguished CTCs isolated from mice xenografted with human prostate cancer cells genetically manipulated for elevated metastatic potential, from CTCs originated in xenografts of wild-type cells (9).

To measure CTCs fitness, we applied mechanical profiling of cells with the supersensitive Peak Force Quantitative Nanomechanical mode of atomic force microscopy (PF-QNM AFM). In this method, a microprobe scans the surface of a live cell by indenting it with a nanoscaled force (Fig. 1A). Physical parameters of the probe’s interactions with the cell during the single nondestructive scan are recorded and translated into maps of nanomechanical parameters: stiffness, deformability, and adhesion (Fig. 1A and B). Stiffness, the most used nanomechanical parameter, describes how much pressure is needed to indent the cell in a reversible (elastic) manner. Stiffness is presented as the object-inherent Young’s modulus in units of pressure (Pascal; Pa). The high Young’s modulus is manifested as high stiffness and low elasticity (Fig. 1A). Stiffness of live cells may range two orders of magnitude from a fraction of kPa to over 50 kPa, however cancer cells are generally less stiff (more elastic) than their noncancerous counterparts (10, 11). The depth of indentation enforced by the probe with a preset force and without cell fracturing is a measure of deformability (length unit: nanometers) that includes elastic and nonelastic components (Fig. 1A). Both stiffness and deformability are crucial for mechanically challenged CTCs (3, 12). We refer to low stiffness accompanied by high deformability as “softness” contributing to mechanical fitness of CTCs. The adhesion (force unit: Newton) is a measure of force needed to lift the tip from the cell surface during the probe withdrawal (Fig. 1A). In our analysis, the inert material (silicon nitrate) tip assures the measure of nonspecific “universal” adhesion. Adhesion of mesenchymal cells is typically much lower than epithelial cells, as expected for mobile cells in contrast to sedentary ones (9, 13). Interestingly, adhesion of CTCs tends to be relatively high, an EMP trait important for cell–cell interactions and cell clustering (5, 8, 14). We use the “high” and “low” designations for parameters in a relative manner, comparing to median values for control, or for special conditions, as specified. In a search for mechanisms distancing biophysical features of CTCs from the primary tumor cells, we turned our attention to cells accompanying CTCs in the bloodstream. It has been reported that CTCs engage in cross-talk with the blood components (15) and interact with platelets (16), myeloid-derived suppressor cells (17), or neutrophils (18). In addition, a presence of macrophage-like cells has been noted in the blood of patients with cancer or model animals (9, 19). We set to explore links between mechanical fitness of CTCs, the presence of accompanying cells and the clinical status of patients with prostate cancer.

Materials and Methods

Additional experimental details are provided in Supplementary Materials and Methods. Sources of reagents and supplies are provided in Supplementary Table S1.

Human subjects

Liquid biopsy samples (blood and void early morning urine) were obtained from male patients following the approved Institution Review Board protocols at the University of Texas Health San Antonio and the Audie L. Murphy Memorial VA Hospital in San Antonio, TX (IRB#HSC20130219H, CTRC#13–0001). Written informed consent was obtained from all subjects in compliance with the Declaration of Helsinki, Belmont Report, US Common Rule following the US

Department of Health and Human Services and the FDA regulations and Good Clinical Practice guidelines. Detailed clinicopathologic information on individual patients is provided in Table 1 and Supplementary Table S2. Morphometric data on blood isolated CTCs and immune cells were collected from images obtained for patients described in Osmulski and colleagues (8).

Isolation, morphometric characterization, and enumeration of cells from liquid biopsies

Exfoliated cellular components were isolated from void urine by centrifugation. Washed cells were stained with specific anti-EpCAM-FITC and anti-CD45-PE antibodies. Then, the cell suspension was captured on glass slides coated with 0.1% branched polyethylenimine for nanomechanical phenotyping. The prostate origin of the urine-isolated EpCAM⁺ cells was confirmed with positive staining for prostate-specific markers PSA and PSMA.

Tumor-associated circulating cells (TACC) were isolated from patients’ blood by size exclusion/microfiltration (8) using ScreenCell CC Filtration Kits. Cells captured on the filters were stained as above with specific anti-EpCAM-FITC or alternatively anti-vimentin-Alexa 488, and with anti-CD163-PE and anti-CD80-Cy5.

Morphometric parameters (footprint) of cells were collected from optical images recorded with Nikon Ti inverted epifluorescent microscope, using ImageJ. Enumeration of TACCs was carried out on recorded optical and fluorescent images.

Cell culture

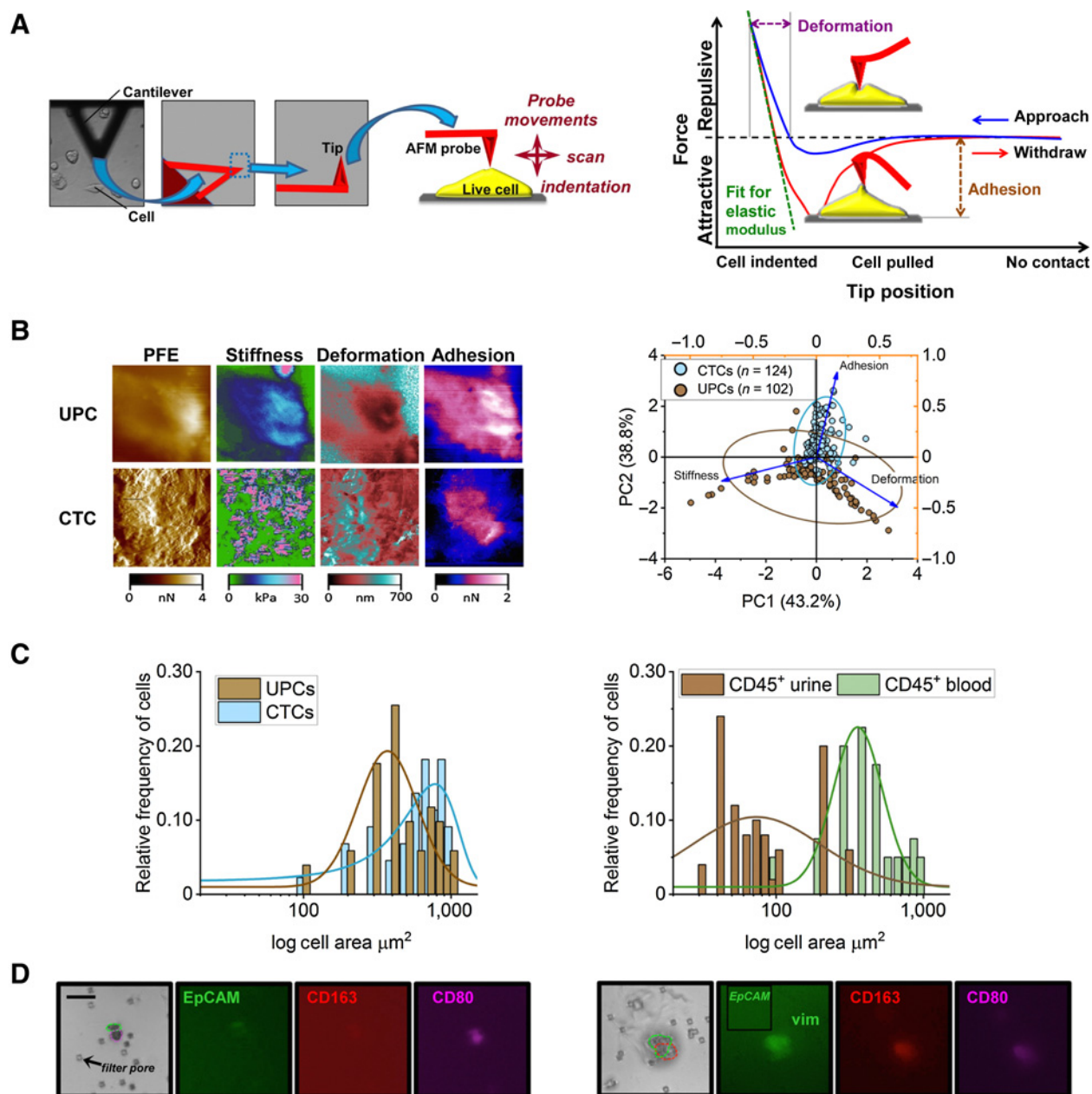
Human prostate cancer cell lines DU145, 22Rv1, and C4-2 (derivative of LNCaP) and monocytoid U937 cells were obtained from ATCC, with authenticity confirmed by the STR Testing Service of the ATCC. The absence of *Mycoplasma* contamination was validated with DAPI staining on regular basis (at least once a month) while maintaining cultures. Nanomechanical profiling was performed on single cells from passages 2 to 4, with cells growing to less than 50% confluence. To assure unequivocal identification of prostate cancer cells in cocultures, we constructed GFP-expressing cells using lentivirus production system (20).

U937 cells were differentiated into M0 macrophages by treatment with phorbol 12-myristate 13-acetate. Naïve macrophages were polarized to M1 (CD80⁺CD163[−]) with lipopolysaccharide and IFN γ , and to M2 (CD80[−]CD163⁺) with IL4 (21). Cells were lifted with non-enzymatic dissociation buffer, counted and added to cancer cells.

Nanomechanical profiling with AFM

CTCs captured on isolation filters, urine prostate cells (UPC) immobilized on PEI-coated slides, and cultured cells surface-growing on dishes were scanned with a Catalyst atomic force microscope (Bruker) mounted on a Nikon Ti inverted epifluorescent microscope. Nanomechanical parameters of cells were collected in the Quantitative Nanomechanical Mapping (PF-QNM) mode of the AFM (8, 9, 22, 23). Before AFM imaging, optical images were recorded for each cell. SCANASYST-AIR probes were used for imaging after their spring constant was determined with the thermal tuning. Cell boundaries were located with peak force error (PFE) AFM images and further verified with height images. Nanomechanical parameters of cells were captured in three separate PF-QNM channels: elasticity (Young’s modulus), deformation, and adhesion. Analysis of these parameters was performed with NanoScope Analysis software v.1.7 (22). Force curves were fit to the Sneddon model, which additionally included adhesion forces and followed the rules proposed by

Osmulski et al.

**Figure 1.**

Urine prostate cells and CTCs present distinct nanomechanical properties and immune cell companions. **A**, Nanomechanical phenotyping. Left, a cartoon representation of a sharp probe mounted on a cantilever scanning the cell by indenting it at each point of tip contact. The leftmost square shows a bright field image of an AFM cantilever mounted over a filter with isolated CTCs. Right, force plots obtained at each point of cell-tip contact allow determination of the nanomechanical phenotype of a cell. **B**, Comparison of typical examples of mechanical properties between a UPC and CTC. Left, each row represents the same single cell, and its mechanical properties are arranged in columns. The first column shows cell topography rendered in a peak force error channel (PFE; Bruker). In this example, the UPC was more stiff, less deformable, and more adhesive than the CTC. Images were false colored using scales covering the data extension. Scale, $10 \times 10 \mu\text{m}$. Right, PCA based on the mechanical phenotype of cells separates population of 122 CTCs ($n = 10$ patients) from 104 UPCs ($n = 11$ patients), with CTCs generally more adhesive than UPCs ($P < 0.0002$ Kolmogorov-Smirnov test; left) and EpCAM⁻CD45⁺ cells captured in blood filtrates (51 cells) and in urine sediments (50 cells) of 21 prostate cancer patients ($P < 0.0001$ Kolmogorov-Smirnov; right). **D**, Examples of TACCs captured on a filter and stained with specific antibodies. Filter pores (6.5 μm diameter) are visible in brightfield images. Left, a cluster of EpCAM⁺ cell and cells positive for the M1 marker CD80. Right, a cluster of cells undergoing EMT (EpCAM⁻vimentin⁺; inset corresponds to the cell-covering area) and cells positive for both CD80 and the M2 marker CD163 ("intermediate macrophages"). See Supplementary Fig. S2B and S2C for examples of single TACCs. Scale bar, 50 μm .

Macrophages Promote Aggressive Mechanical Phenotype of CTCs

Table 1. Clinicopathologic status of 23 patients whose blood (33 samples/visits) was used for tumor-associated circulating cell isolation and characterization by nanomechanical and immunocytochemical profiling.

Sample number (visit)	Disease spread (update)	PSA at draw (ng/mL)	Treatments: primary, secondary, tertiary, quat.	Stage at diagnosis, prostatectomy	Gleason: diagnosis, prostatectomy	Months from prostatectomy	BCR	Months from ADT	CS/CR (update)
1 ^a	Regional	0.24	Surgery, ADT	cT2b, Nx, Mx pT3a, N1, Mx, R1	4 + 5, 5 + 4	35	Yes	-5	CS (CS)
2 ^a	Regional	0.18	Surgery, ADT	cT2b, Nx, Mx pT3a, N1, M0, R0	4 + 3, 4 + 4	25	Yes	3	CS (CS)
3 ^a (1)	ND	0.04	Surgery, radiation	cT1c, N0, M0 pT3b, N0, MX	3 + 4, 4 + 3	10	No	None	CS (CS)
4 (2)	ND	0.10	Same	Same	Same	17	No	None	CS (CS)
5 ^a	ND	0.14	Surgery	T1c, Nx, Mx pT2c, pNx, Mx	3 + 3, 3 + 3	140	No	None	CS (CS)
6 ^a	ND	14.99	ADT	T2b, N0, M0 NA	4 + 4, NA	None	No	0	CS (CS)
7 ^a (1)	M1b	704.3	ADT, chemo, ADT, radiation	cT4, N1, M1 NA	4 + 5, NA	None	No	0	CS (CR)
8 (2)	M1b	NA	Same	Same	Same	None	No	6	CS (CR)
9 ^a	ND (M1b)	37.17	ADT, radiation	cT3	4 + 3, NA	None	No	0	CS (CS)
10 ^a	M1a and M1b	4.2	ADT, surgery, radiation	NA	4 + 4, 4 + 5	44	D	0	CS (CS)
11 ^a	Regional	2.94	Surgery, ADT	cT2b, N0, M0 pT3b, N1, MX	4 + 5, 4 + 5	35	Yes	0	CS (CS)
12 ^a	ND	1.36	Surgery, ADT, radiation	NA, pT3a/b, R1, N0, Mx	4 + 3, 4 + 3	18	Yes	0	CS (CS)
13 (1)	ND	0.51	Surgery, radiation, ADT	cT2c, N0, M0	4 + 5, 3 + 4	32	Yes	0	CS (CR)
14 (2)	ND	NA	Same	pT3b, N0, Mx Same	Same	38	Yes	6	CR
15	Regional	0.06	Surgery, ADT	cT1c, N0, M0 pT3b, N1, M0, R1	3 + 4, 4 + 4	7	No	0	CS (CS)
16	Regional	1.83	Surgery, radiation, ADT, chemo	NA, pT2b, N1	4 + 5, 4 + 5	29	D	25	CS (CS)
17	M1a and M1b	102	Chemo, ADT, radiation	NA	NA	None	No	>24	CR
18 (1)	M1b	12.39	ADT, radiation, chemo	cT3, N1, M1 NA	4 + 5, NA	25	Yes	28	CS (CS)
19 (2)	M1b	NA	Same	Same	Same	28	Yes	31	CS (CS)
20	ND	0.24	Surgery, radiation, ADT	cT2a, N0, M0 pT3b, NX, MX	3 + 4, 4 + 4	45	Yes	None	CS (CS)
21 (1)	M1a	4.68	ADT, radiation	NA	3 + 4, NA	45	No	45	CS (CS)
22 (2)	M1a	NA	Same	Same	Same	54	No	54	CS (CS)
23 (1)	ND	7.22	Radiation, ADT	NA	3 + 4, NA	27	Yes	0	CS (CS)
24 (2)	ND	NA	Same	Same	Same	37	Yes	10	CS (CS)
25 (1)	ND	0.96	Radiation, ADT	pT3a, N1, M0	4 + 5, NA	120	Yes	0	CS (CS)
26 (2)	ND	NA	Same	Same	Same	124	Yes	4	CS (CS)
27 (1)	ND	18.3	Radiation, ADT	T1c, Nx, Mx	3 + 3, NA	72	No	0	CS (CS)
28 (2)	ND	NA	Same	Same	Same	75	No	3	CS (CS)
29 (1)	M1a	0.05	Surgery, ADT	NA, pT3b, N1, M0, R1	3 + 4, 4 + 4	1	D	0	CS (CS)
30 (2)	M1a	NA	Same	Same	Same	4	D	3	CS (CS)
31 (1)	M1a	43.8	ADT, radiation	cT1c, N1, M0	4 + 5, NA	0	No	0	CS (CS)
32 (2)	M1a	M1a	Same	Same	Same	4	No	7	CS (CS)
33	ND	9.66	Radiation, ADT	cT2b, Nx, Mx	3 + 4, NA	156	Yes	0	CS (CS)

Note: The CS/CR and metastasis status at the time of visit/blood draw is presented. The "update" refers to information obtained at least 6 months after the visit (in the case of patient no. 1, after the start of ADT). (1) and (2) with consecutive numbers denote blood samples obtained during 1st and 2nd visits of the same patient (10 patients).

Abbreviations: BCR, biochemical recurrence; CS/CR, castration sensitive/resistant; chemo, chemotherapy; D, PSA always detectable; NA, no data available; ND, not detected; prostatectomy, surgery and/or radiotherapy; quat., quaternary treatment.

^aCTCs used for comparison with urine prostate cells (Supplementary Table S1).

Osmulski et al.

Sokolov (8). Mode values of the mechanical parameters for individual cells were calculated from the corresponding distribution histograms.

Proteomic analysis with cytometry by time-of-flight

Cells cultured/cocultured as above were harvested for single cells with trypsin and processed for cytometry by time-of-flight (CyTOF) running. The cells were stained with metal-conjugated antibodies (Fluidigm; Supplementary Table S3). CyTOF data were clustered and visualized using t-distributed stochastic neighbor embedding (t-SNE) algorithm based on normalized expression levels (Z-score) of markers of protein expression with phenotypically related cells clustered together.

Statistical analysis

Hierarchical cluster analysis with corresponding heat maps and principle component analysis of the mechanical properties of the cells, and cell enumeration was performed using OriginPro 2020 with additional assistance from Statistica (TIBCO). Binary logistic regression was applied to predict odds of cases (OriginLab). Kolmogorov–Smirnov test was used to compare data distributions of two unmatched groups. Normal distribution was checked with Kolmogorov–Smirnov and Anderson–Darling tests. Cell viability among circulating tumor cells and mechanical properties of cancer cells cocultured with macrophages were compared using two-tailed Student *t* test or one-way ANOVA. To test whether Pearson correlation coefficients were significantly different from 0, we applied the two-tailed *t* test. For comparison of groups with normally distributed data, the *post hoc* Tukey test was summoned. If the normality test failed, the nonparametric Kruskal–Wallis test was applied and the Dunn test was used for between groups comparison.

When the assumption of equal SD was not met and group sizes were substantially different, the Brown–Forsythe test was called. Then, the Dunnett T3 test was used for *post hoc* analysis. Statistically significant differences between populations were assumed if $P < 0.05$. General descriptive statistics was completed with OriginPro 2020 and Graph-Pad Prism 9.0.

Results

Tumor-shed cells in blood and urine display distinct nanomechanical phenotypes and coisolate with distinct populations of immune cells

In the case of prostate tumors, cancer cells are shed into the blood as CTCs and also to urine as UPCs with a biomarker potential (24). Both CTCs and UPCs are exposed to damaging fluid shear stress; however only CTCs may act as “seeds of metastasis,” while UPCs inevitably perish. We decided to compare nanomechanical phenotypes of the two classes of cells released from a tumor to test their adaptation to the flow challenge.

Microfiltration of blood collected from prostate cancer patients yielded filter-settled large cells, many of them EpCAM⁺ (8). Large EpCAM⁺ cells were also abundant in urine sediment collected from patients with prostate cancer. AFM analysis was performed on cells positive for prostate-specific markers PSA/PSMA (Table 1; Supplementary Table S2; Fig. 1B). The patient cohort was comprised of high-risk patients with local disease and patients with low-volume metastatic spread (Table 1; Supplementary Table S2). With principal component analysis (PCA), we found that cell adhesion showed the most striking difference among these exfoliated cells. CTCs appeared 5-fold more adhesive than UPCs (Fig. 1B). Analysis of stiffness and deformability revealed a remarkable diversity among UPCs: One class

of UPCs was not significantly different from CTCs, whereas the other class was almost seven times stiffer than CTCs (Fig. 1B). We speculate that those stiff UPCs may undergo apoptosis, consistently with data reporting cell death accompanying increase in the Young's modulus (25). High softness and low adhesion are known mesenchymal hallmarks of aggressive cancer cells, and the soft, nonadhesive class of UPCs embodied these traits. However, the majority of CTCs retained epithelial adhesion (14). At the same time the CTCs displayed mesenchymal properties for softness. Consistently, high adhesion and softness were distinctive “mechanical fitness” features of the most aggressive prostate cancer CTCs in our previous studies (8).

Both CTCs and UPCs are shed from the tumor; however only CTCs displayed the unique mechanical fitness phenotype. CTCs may originate from metastatic sites, not only the primary tumor as assumed for UPCs (1). Only 2 of 10 patients used for this study were diagnosed with distant spread (Table 1) and phenotypes of their CTCs did not form a separate class in the population of all CTCs (Supplementary Fig. S1A). In a search for other features distinguishing blood-isolated and urine-isolated cells, we turned our attention to immune cells accompanying UPCs and CTCs. Both blood retentates and urine sediments contained EpCAM⁺ cells but also numerous EpCAM[−] cells positive for pan-leukocyte marker CD45 (leukocyte common antigen; Supplementary Fig. S1B). Morphometric analysis of a random sample of light/fluorescent microscopy images of these cells revealed that EpCAM⁺ cells were predictably large in both blood and urine preparations. Footprints of these cells corresponded to squares with average lengths of 24 μm (44 CTCs; range of lengths 10 μm–32 μm) or 21 μm (51 UPCs; range of lengths 8 μm–30 μm), well within morphologic parameters reported for CTCs (19). Population of CTCs with larger footprints was more numerous than a similar population in UPCs (Fig. 1C). This may reflect the high content of CTC pairs in blood retentates, consistent with high adhesiveness of CTCs as compared with UPCs. Such cell pairs are customarily counted as single objects in FDA-approved diagnostic/prognostic enumerations of CTCs. In turn, footprints of the immune cells found in urine sediments were rather small (average diameter 10 μm, range 6 μm–18 μm; Fig. 1C) corresponding to typical leukocytes with expected diameters ranging from 7 μm to 15 μm (26). Instead, blood-derived EpCAM[−] CD45⁺ cells had an average diameter of 23 μm, (range: 16 μm–25 μm; Fig. 1C). The observed difference in size distribution could not be attributed solely to the expected enrichment of blood retentates in large cells, as partitions of tumor-to-immune cells were very similar, close to 1:1, in preparations recovered from the two types of liquid biopsies (see caption to Fig. 1C). However, large immune cells were absent in urine.

CTCs are accompanied by immune cells bearing surface markers of macrophages

The exceptionally large immune cells copurifying with CTCs may have corresponded to macrophages (19). We designated all cells isolated by microfiltration as “tumor-associated circulating cells” (TACC) and attempted to classify them. The presence of TACCs was unique for the blood of cancer patients (Supplementary Fig. S1C): Filtration of the blood sample of a healthy donor yielded neither immune nor epithelial-like cells, with scarce fragments of exfoliated vessel lining cells as the only filter-bound material (Supplementary Fig. S1D). We chose the following surface markers to characterize TACCs: epithelial marker EpCAM, EMT-indicating vimentin (27), macrophage scavenger receptor CD163 expressed by anti-inflammatory macrophages of M2 type of polarization, and the marker of M1 proinflammatory macrophages, the T-lymphocyte activation antigen CD80 (28). According to immunocytochemical clues, we

Macrophages Promote Aggressive Mechanical Phenotype of CTCs

classified the presumably tumor-derived cells as EpCAM⁺ CTCs (EpCAM⁺/vimentin^{+/-}/immune markers⁻) or EMT CTCs (EpCAM⁻/vimentin⁺/immune markers⁻; Fig. 1D; Supplementary Fig. S1C). CTCs were sometimes found in clusters with other CTCs (homotypic, “homo-clusters”) or with immune cells (heterotypic, “hetero-clusters”; Fig. 1D). In turn, the non-CTC TACCs presented macrophage-like signatures and could be assigned as M1-like macrophages (EpCAM⁻/vimentin⁻/CD163⁻/CD80⁺), “intermediate” macrophages (EpCAM⁻/vimentin⁻/CD163⁺/CD80⁺), and M2-like macrophages (EpCAM⁻/vimentin⁻/CD163⁺/CD80⁻; Fig. 1D; Supplementary Fig. S1C). The CD163 surface marker that was prominent in immune TACCs is commonly found on cancer-promoting tumor associated macrophages (TAM; refs. 29–31). TAMs serve as an important component of tumor microenvironment with immunoprotective, proangiogenic and invasiveness-supporting actions (31). Although usually referred as M2-like, TAMs often defy the canonical M1–M2 polarization axis. The CD163⁺CD80⁺ signature referred here as “intermediate” may indicate TAMs of M2d-like type (31–33). TAMs may also display M1-like phenotype with detectable CD80 surface marker, raising the possibility that macrophages copurifying with CTCs are circulation-born TAMs (34).

Mechanical fitness of CTCs correlates with enumeration of TAM-like immune cells

To track possible links between nanomechanical phenotypes and the presence of distinctive macrophages, we performed a comprehensive mechanical and immunocytochemical analysis of TACCs isolated from 33 blood samples obtained from 23 patients with high-risk prostate cancer with local disease or with low metastatic tumor burden, undergoing diverse treatments, including androgen deprivation therapy/ADT (Table 1). Two blood samples obtained during two separate visits were analyzed for 10 patients (Table 1). Clinical information was updated on the basis of changes in castration sensitivity or development of metastasis several months after the initial visit (Table 1). The total of 514 single EpCAM⁺ or vimentin⁺ CTCs were interrogated with AFM. The filter-retained 4,127 TACCs were analyzed with immune staining (Fig. 1D; Supplementary Fig. S1B). The results of nanomechanical profiling are presented in Fig. 2 and Supplementary Table S4). Hierarchical cluster analysis followed by PCA indicated the presence of four categories of CTCs distinguished by their nanomechanical phenotypes: 1, high stiffness; 2, moderate stiffness, deformability, and adhesion; 3, very soft (low stiffness, high deformability); and 4, very adhesive (Fig. 2A). Then, we determined the partition of each category for all patients’ CTC samples. From our previous study, softness and adhesion were deemed hallmarks of aggressive CTCs (8). On this basis, we ordered the samples according to contribution of “best fit” categories 4 and 3, from lowest to highest contribution (Fig. 2B). Next, we aligned the partition and enumeration of distinct kinds of TACCs with this “fitness chart” of patients’ CTCs (Fig. 2C; Supplementary Fig. S2). Enumeration of EpCAM⁺ CTCs generally decreased with increasing fitness (Fig. 2C), with no clear trend for enumeration of EMT CTCs (Supplementary Fig. S2). Enumeration of total TACCs, M1-like, intermediate as well as total macrophages increased with increasing fitness of CTCs, with no clear trend for enumeration of M2-like macrophages (Fig. 2C; Supplementary Fig. S2). When partition of distinct TACCs were considered, the decreasing contribution of EpCAM⁺ CTCs and increasing contribution of total macrophages with the increasing fitness of CTCs were apparent (Fig. 2B).

In a search for formal representation of the trends we turned to general linear regression analysis. We translated the partition of

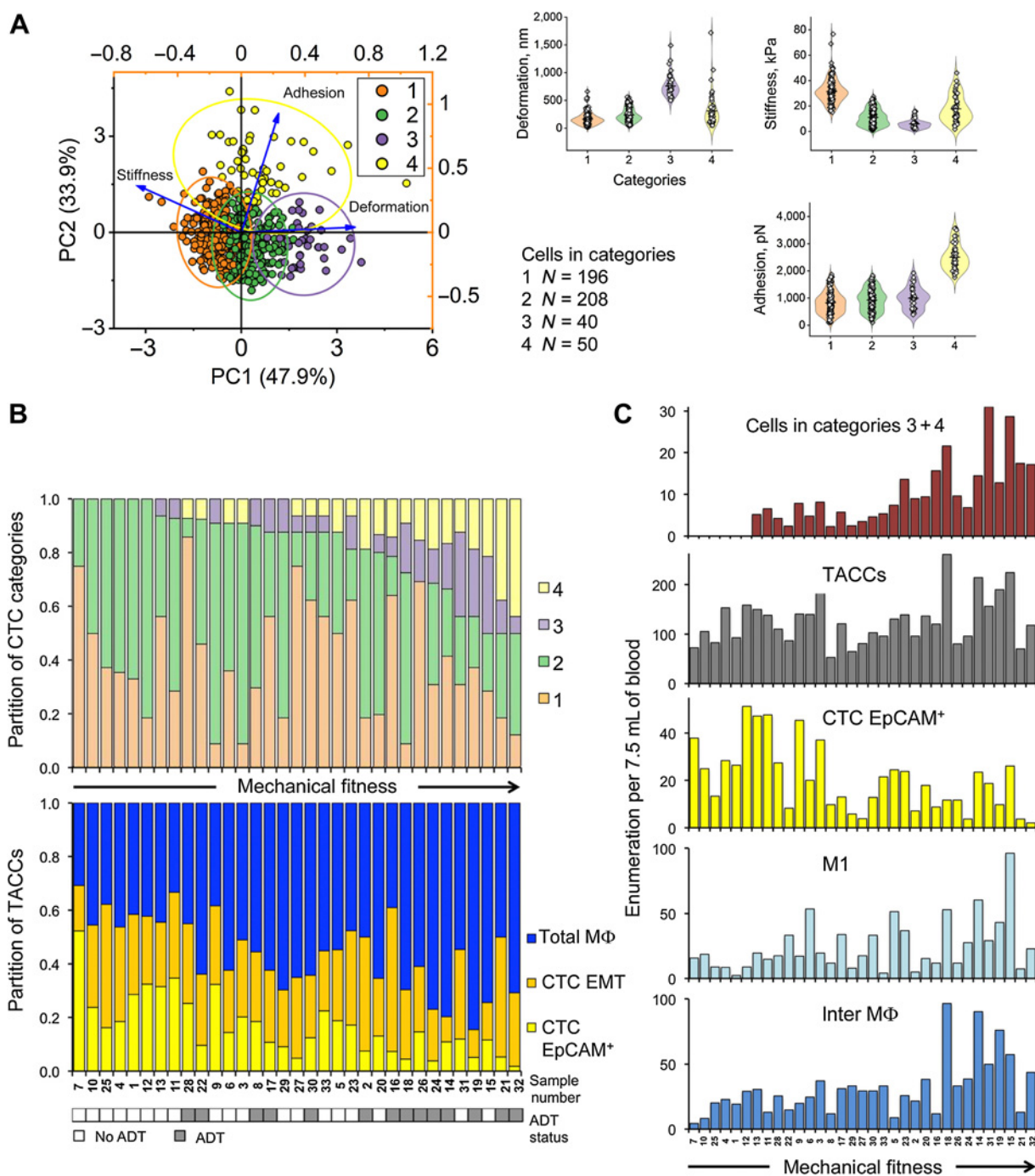
mechanical phenotype categories (Fig. 2A and B) into enumeration of the categories in the total CTC population. The strongest correlations are presented in Fig. 3 and Supplementary Fig. S3A and S3B. Apparently, enumeration of category 3 (well-fit, very soft cells; Fig. 2A) correlated with enumeration of intermediate macrophages (Fig. 3A). In turn, enumeration of category 2 (Fig. 2A) correlated with enumeration of M2-like macrophages (Fig. 3B). We may speculate that cells from category 2 were trained specifically by M2-like macrophages to attain fitness. Enumeration of well-fit, very adhesive cells from category 4 (Fig. 2A) only weakly correlated with enumeration of M1-like and intermediate macrophages (Supplementary Fig. S3A and S3B, respectively). Possibly, these CTCs were already sufficiently prepared for circulation and did not strongly rely on the presence of macrophages for survival. Enumeration of the poorly fit category 1 (very stiff cells; Fig. 2A) did not significantly correlate with any macrophage enumerations (Supplementary Fig. S3C). These cells were likely destined for apoptosis without evidence of positive or negative intervention from macrophages.

Next, we attempted to search for patterns of clinical conditions in our CTCs fitness chart. Apparently, CTCs isolated from patients that never underwent hormonal therapy (pre-ADT) tended to display rather low or moderate fitness (Fig. 2B). This trend was supported by a cluster analysis of nanomechanical parameters and enumerations of TACCs as variables: A separate cluster was formed by pre-ADT cases (Supplementary Fig. S4; Table 1). Strikingly, only in this cluster all patients remained castration sensitive for the study duration (Supplementary Fig. S4; Table 1).

To follow on the effects of ADT on CTCs, we compared the nanomechanical parameters and enumerations of TACCs from patients before and after ADT treatments (Fig. 3C and D). Strongest correlations observed in pre-ADT samples included: deformability with enumeration of intermediate macrophages (positive), adhesion with enumeration of M1 and intermediate macrophages (positive), and stiffness with enumeration of M2-like macrophages (negative; Fig. 3C). High deformability and adhesion, and low stiffness were commonly observed in well-fit CTCs (Fig. 2A). Generally weaker correlations were noted for post-ADT samples (Fig. 3C). Next, we considered correlations between enumeration parameters (Fig. 3D). The strongest positive correlations were observed between intermediate and M1-like macrophages in post-ADT cases, possibly suggesting potentially dangerous posttherapy recruitment of monocyte-derived macrophages in circulation (Fig. 3D). Intermediate macrophages might be expected to cluster with pre-ADT CTCs taking into account the respective positive correlation (Fig. 3D). The occasionally observed negative correlations between enumerations of single TACCs and clusters may indicate that clusters were broken during TACCs isolation (Fig. 3D). Taken together, the aggressive nanomechanical phenotypes of well-fit CTCs were accompanied by the high enumeration of macrophages, a trait particularly well discerned in patients who were not previously treated with ADT.

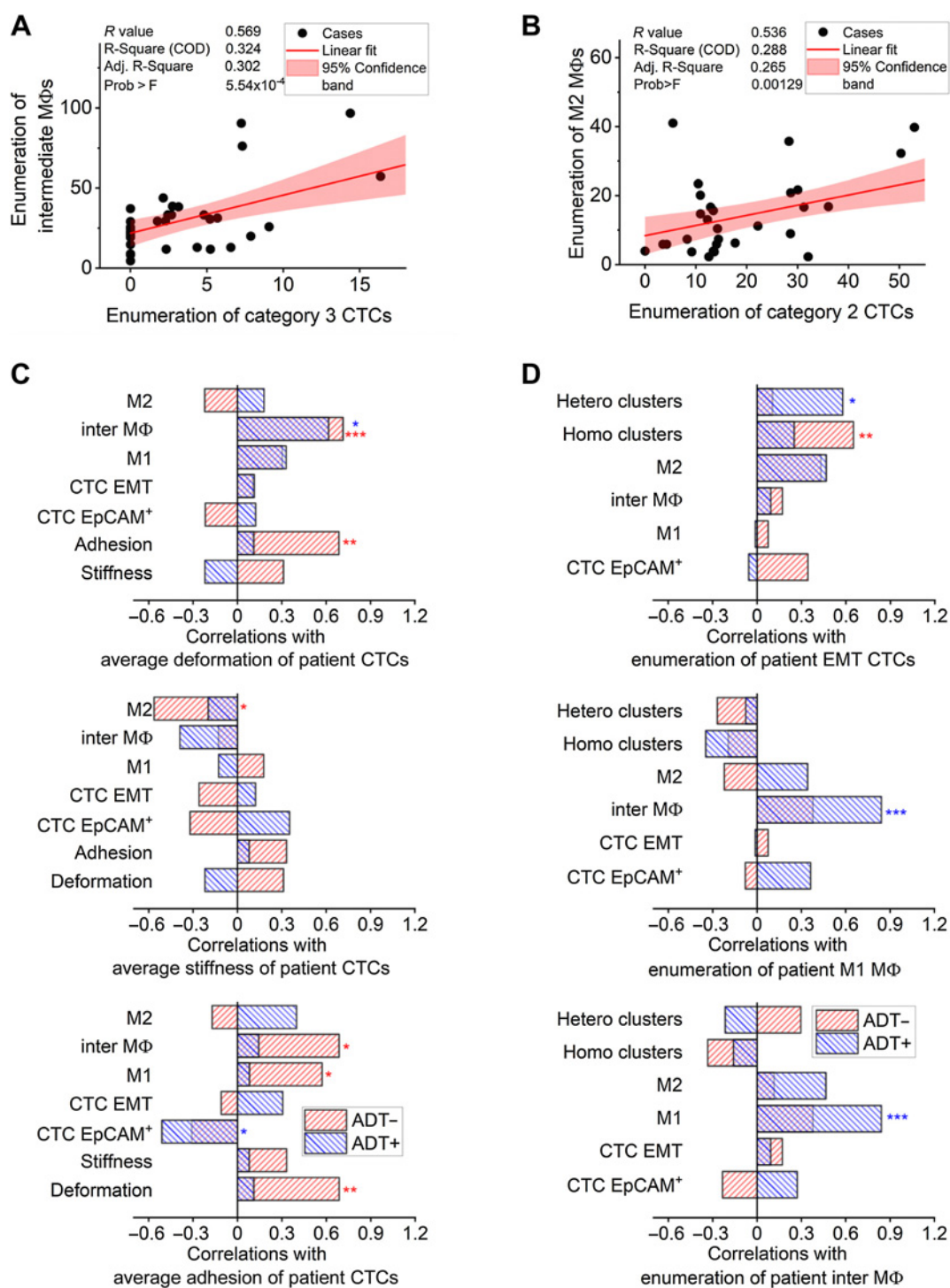
The status of ADT and castration sensitivity/resistance was not the only clinical parameters trending with mechanical fitness of CTCs or enumeration of TACCs. The order of cases in CTCs fitness chart did not follow the reported metastatic spread (Supplementary Fig. S2). Instead, we focused on adhesion as the most distinctive parameter distinguishing CTCs from tumor-shed cells such as UPCs. Next, we performed binary logistic regression using the average adhesion of CTCs for each patient and their corresponding disease spread status (Table 1; Supplementary Table S2). We noticed a correlative trend ($P = 0.22$) in high cell adhesion with metastasis. We posit that the increase in CTC adhesion may portend a poor prognosis with a higher

Osmulski et al.

**Figure 2.**

Mechanical phenotyping of 494 CTCs isolated by microfiltration from 33 blood samples from 23 prostate cancer patients. **A**, Left, hierarchical cluster analysis followed by PCA of stiffness, adhesion, and deformation revealed the presence of four categories of cells. Right, violin plots of the mechanical properties of cells identified in each category. Categories 3 and 4 contain cells with high mechanical fitness. Black horizontal lines represent averages. **B**, Partition of the four categories of cells in the 33 analyzed blood samples (top) and partition of three classes of TACCs (bottom). The samples (patient number-visit number) were ordered according to the relative abundance of CTCs linked to mechanical category 4 and category 3 (best-fit cells). **C**, From the top: enumeration (cells per 7.5 ml of blood) of cells in categories 3 and 4, all TACCs, EpCAM⁺ CTCs, CD80⁺ macrophages (M1), and CD163⁺CD80⁺ macrophages ("inter"). The samples were ordered as in **B**, according to mechanical fitness.

Macrophages Promote Aggressive Mechanical Phenotype of CTCs

**Figure 3.**

Nanomechanical parameters of patient-isolated CTCs correlate with enumerations of selected types of macrophages. **A** and **B**, Enumerations of intermediate macrophages (**A**) and M2-like macrophages (**B**) correlate with abundance of well mechanically fit (category 3) or moderately fit (category 2) CTCs, respectively (general linear regression). Both correlations are statistically significant with $P < 0.001$ (**A**) and $P < 0.01$ (**B**), based on t test. In columns, **C** and **D**, Pearson r correlations of the parameters with (from the top) deformation, stiffness, and adhesion (**C**) and correlations of TACC enumerations with (from the top) enumeration of EMT CTCs, M1 macrophages, and intermediate macrophages (**D**). Respective correlations with enumeration of EpCAM⁺ CTCs and M2 macrophages did not exceed 0.5/–0.5 and are presented in Supplementary Fig. S3. Statistically significant correlations are based on t test. *, $P < 0.05$; **, $P < 0.01$; ***, $P < 0.001$.

Osmulski et al.

risk for development of metastasis. Importantly, other mechanical parameters did not show any such trend. This observation underscored a special significance of cell adhesion for the mechanical fitness and presumed survival skills, resilience, and ultimately invasiveness of CTCs.

Cultured prostate cancer cells respond to coculture with model macrophages with improved mechanical fitness

To recapitulate the putative productive interactions between tumor cells and macrophages, we investigated cell coculture models. We chose three prostate cancer cell lines of distinct lineages and invasiveness: 22Rv1, DU145, and C4-2 (Supplementary Table S5). The cells

cultured alone were mechanically diverse; however, at least subsets of their nanomechanical phenotypes were very similar to phenotypes observed for CTCs (Fig. 4A; Supplementary Tables S4 and S5). The spread of mechanical parameters was the largest in control 22Rv1 cells, likely due to their mixed genetic background. In turn, high adhesion was the most distinctive feature of DU145 cells. C4-2 cells were soft and not very adhesive, suggesting mesenchymal-like phenotype expected in highly invasive tumor cells (Fig. 4B; Supplementary Tables S4 and S5). When cells from each of the lines were separately classified with cluster analysis into four categories according to relative mechanical fitness, 22Rv1 cells had approximately equal representation of categories with low to high relative fitness (Fig. 5A), in DU145 cells the

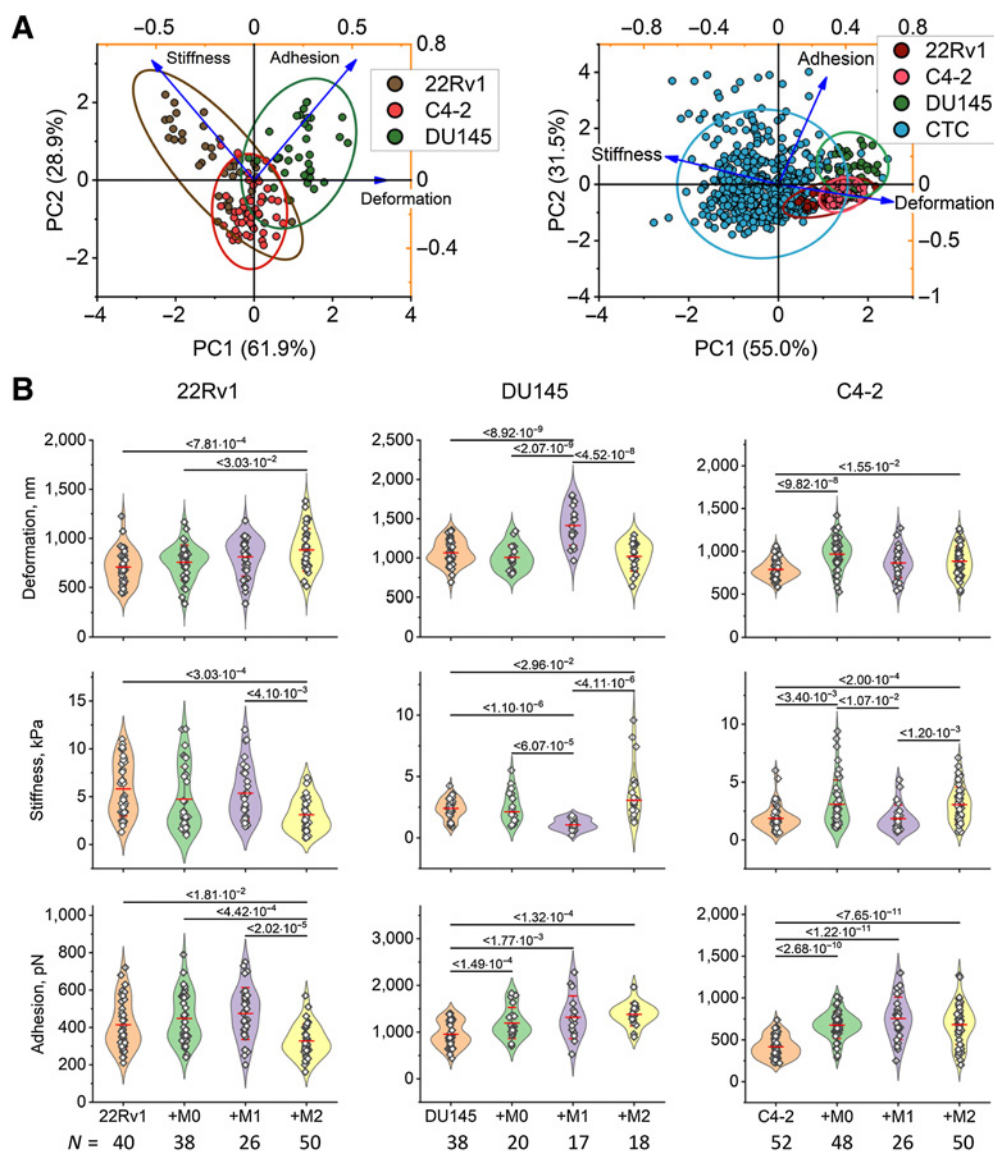
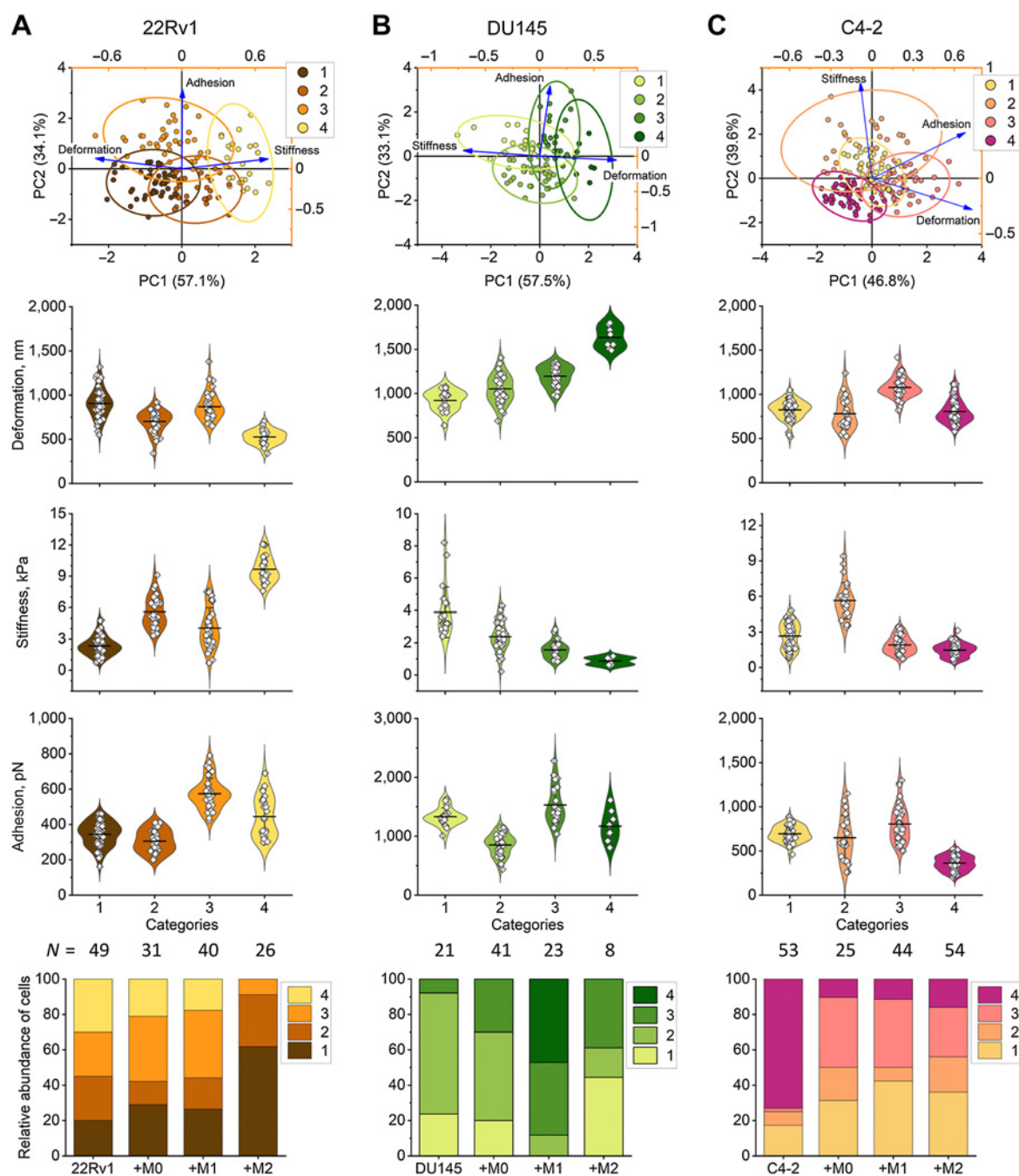


Figure 4.

Human cultured prostate cancer cells display cell line-specific mechanical properties that are comparable in part with patient-isolated CTCs. The mechanical parameters of model prostate cancer cell lines specifically respond to coculture with model macrophages. **A**, PCA of mechanical properties of prostate cancer cell lines (left) and contrasted with CTCs (right). Properties of the control prostate cancer cells overlap with the most deformable and adhesive CTCs. A total of 40 22Rv1, 38 DU145, and 52 C4-2 cells were compared with 514 CTCs (total 644 cells). **B**, Violin plots of nanomechanical parameters of control prostate cancer cell lines and cells cocultured with model macrophages of distinct polarization. Listed are statistically significant differences based on one-way ANOVA analysis.

Macrophages Promote Aggressive Mechanical Phenotype of CTCs

**Figure 5.**

Cultured prostate cancer cells exhibit distinct mechanical phenotypes in response to coculture with model macrophages. Hierarchical cluster analysis followed by PCA was performed for each control cell line [22Rv1 (**A**), DU145 (**B**), and C4-2 (**C**)] and cells cocultured with macrophages. The increased abundance of mechanically well-fit cells is a common attribute of cancer cells exposed to macrophages. In columns from the top: PCA of nanomechanical parameters of single cells; violin plots of parameters spread in the categories shown with PCA; and relative abundance of the categories in control and cocultured cells. Cells in categories with high adhesion and/or low stiffness are considered mechanically well fit.

moderate-fitness category prevailed (**Fig. 5B**), whereas the majority of tested C4-2 cells were highly fit in terms of softness, however moderately prepared for potential cell-cell interactions (**Fig. 5C**). In summary, cultured cells presented nanomechanical profiles comparable to CTCs, albeit more extreme than the majority of CTCs

(**Fig. 4A**). Such diversity positioned these cultured cell lines as good models representing prostate cancer cells spanning different clinical stages of propensity for metastatic tumor spread.

In the next series of experiments, we cocultured the model prostate cancer cells for 24 hours with *in vitro* differentiated and polarized

model human macrophage-like cells derived from a monocytic U937 cell line. All prostate cancer cells were expressing GFP for their unequivocal identification in coculture. We used differentiated, non-polarized M0-like naïve macrophages; M1-like polarized or M2-like polarized U937-derived macrophages in a 1:1 ratio with cancer cells. Single cancer cells were phenotyped with AFM. Clearly, coculture with all types of model macrophages affected nanomechanical profiles of prostate cancer cells; however extent and direction of changes depended both on the polarization of immune cells and the cancer cell line (Figs. 4 and 5). The phenotypes of 22Rv1 cells were affected the most by M2-like macrophages, with significantly softer but less adhesive cells after coculture. The category 4 of stiff cells disappeared entirely from cocultures with M2-like macrophages. Coculture with M0 and M1-like macrophages was accompanied by a moderately increased participation of soft and adhesive cells (Figs. 4A and 5A). Interestingly, coculture with M1-like macrophages induced the most pronounced changes in nanomechanical phenotype of DU145 cells: Categories of very soft as well as soft and adhesive cells prevailed. Still, adhesion of tumor cells systematically increased with not only M1- but also M0- and M2-like macrophages as partners in coculture (Figs. 4B and 5B). In turn, the C4-2 cells responded similarly to the presence of all types of macrophages with attaining higher deformability and adhesion (Figs. 4B and 5C). In general, the coculture with polarized macrophages seemed to have more pronounced effects on nanomechanical phenotypes than coculture with naïve macrophages (Figs. 4 and 5; Supplementary Fig. S5A–S5C). Summarizing, coculture with model macrophages consistently promoted fitness of model cancer cells: high adhesion, high deformability, and low stiffness, with majority of the cells still remaining within the range of the mechanical similarity to CTCs (Figs. 4B and 5; Supplementary Fig. S5D).

Coculture of DU145 cells with macrophages results in EMP

To understand molecular mechanisms that promote changes in nanomechanical phenotypes, we conducted proteomic analysis using GFP-DU145 cultured alone (control) or with M0, M1, or M2 model macrophages. DU145 cells responded to the coculture with the most pronounced AFM-detected shifts (Figs. 4B and 6B; Supplementary Fig. S5). The cancer cells were subjected to CyTOF with E/M panel of 16 antibodies (Fig. 6A–C; Supplementary Table S3). t-Distributed Stochastic Neighbor Embedding (t-SNE) projections of treatments of DU145 cells are presented in Fig. 6B. Each of four treatment populations was further divided into subpopulations with distinct proteomic marker profiles for eight mesenchymal and seven epithelial markers (Fig. 6B). As evident in Fig. 6C, both control and cocultured cells displayed mixed E/M profiles with expression of both epithelial [EpCAM, cytokeratins, ZO2 (TJP2)] and mesenchymal [β -catenin, vimentin, N-cadherin, and Slug (SNAI2)] markers. However, cumulative analysis revealed that contribution of the mesenchymal markers systematically decreased upon coculture with macrophages, with polarized macrophages triggering stronger shifts than M0-like cells (Fig. 6D and E). These changes mirrored those in nanomechanical phenotypes of DU145 cells, where polarized macrophages introduced stronger fitness-promoting trends than naïve macrophages (Figs. 4B and 6B, Supplementary Fig. S5D). Apparently, the mechanical fitness was supported by a partial reversion from an advanced mesenchymal to a more-epithelial phenotype. A striking example of the reversion is a decreasing level of TWIST and N-cadherin accompanied by an increasing level of E-cadherin in DU145 cells cocultured with M2 macrophages (Fig. 6C). In the course of standard EMT, TWIST is repressing transcription of E-cadherin (35). Contribution of oncogenic signal components followed the EMP profile as well: Certain markers

such as VEGFR1 (FLT1) or WNT5A were at the highest in control DU145 cells; however, some others, most notably SMAD2, EGFR and P-ERK1/2 attained high levels in the cocultured cells (Fig. 6F). It seems that cancer cells educated by macrophages may forgo the certain features of invasive mesenchymal phenotype in favor of the EMP promoting mechanical endurance especially important for CTCs. Maintaining the high adhesion and high softness appears to be the most distinctive manifestation of CTC-relevant intermediate E/M state.

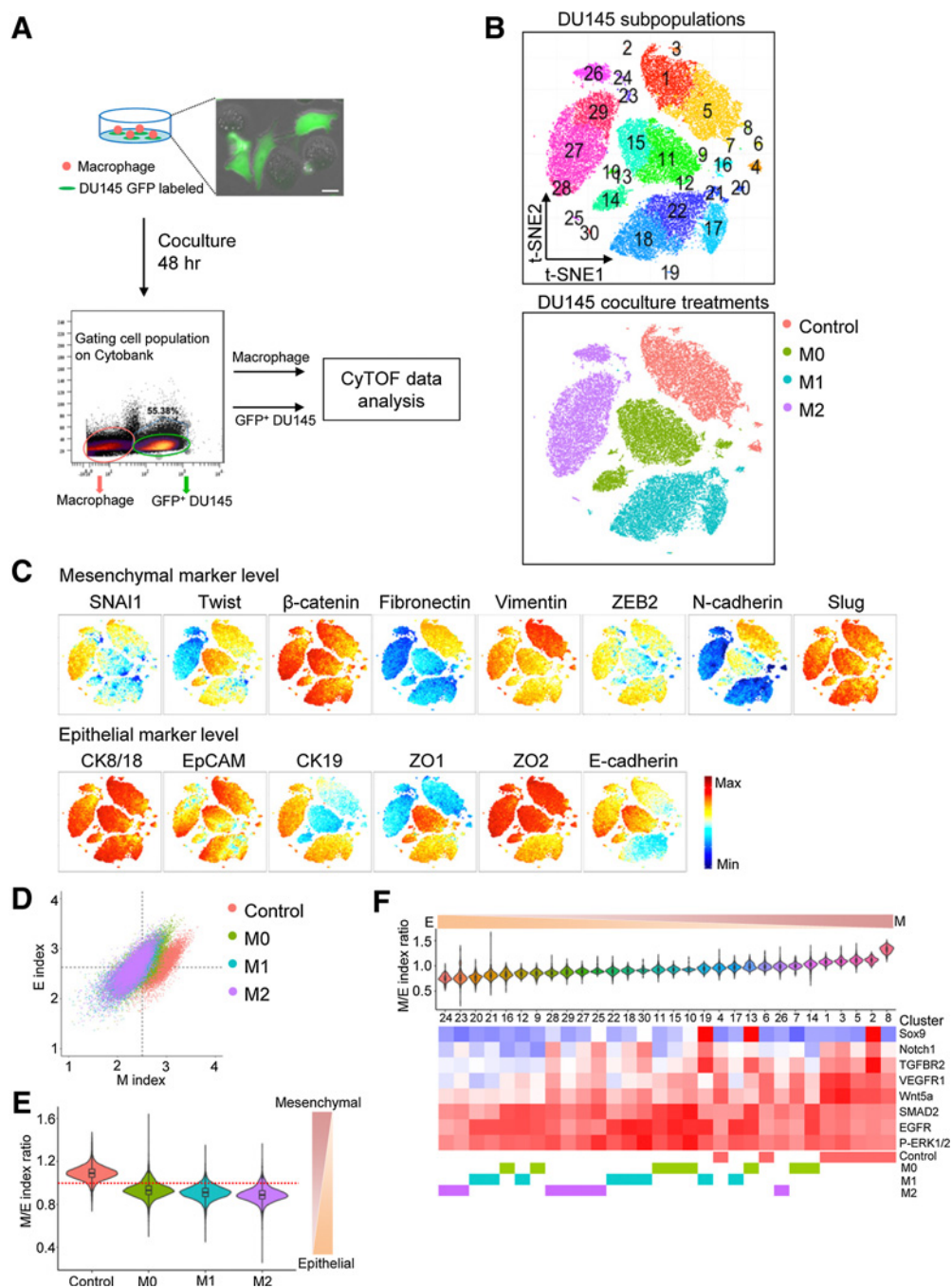
Discussion

Mechanical phenotypes of cells are tuned to their physiologic function: rigidity of osteocytes, and deformability of erythrocytes providing examples of extreme adaptations (11). Changes in mechanical properties of cells are often very early and sensitive signs of physiologic changes in the tissue environment (10, 11). Prostate tumors, as other epithelial-origin tumors, are overcrowded structures. Inhabitant cells are mechanically labile to survive the intertumor pressure and many cells readily escape the tumor. The escapees may be a random set of cells positioned close to the outside routes: the urethra, the lymph vessels or the blood vessels or they could be uniquely prepared for dissemination. Our comparison of mechanical phenotypes of prostate tumor cells shed to urine (UPC) and to blood (CTC) suggests the latter. Both cell populations experience fluid shear stress of similar magnitudes when comparing liquid flow in urethra and veins (36–38). However, mechanical properties of soft and non-adhesive UPCs reflected their aggressive tumor origin, whereas CTCs were distinguished by high adhesion, a feature we observed before in aggressive CTCs (8). We concluded that while UPCs represent a random sample of tumor cells, the CTCs might be specifically adapted for dissemination. Since only CTCs copurify with large numbers of immune cells bearing markers of TAMs, we hypothesized that tumor-escaping CTCs and TAMs are uniquely linked for promotion of metastatic spread.

In a search for putative connections between aggressive traits of CTCs and the presence of macrophages, we analyzed the nanomechanical phenotypes of the CTCs and compared them with abundance of the macrophages. Following our previous works with prostate cancer CTCs, we considered the elevated softness and adhesion as biomarkers of aggressive disease and hallmarks of survival-promoting mechanical fitness (8). We found the enumeration and abundance of EpCAM⁺ CTCs to be low in samples with the best-fit cells. This pointed at a shortcoming of affinity-based CTC isolation methods that neglect EMT-undergoing EpCAM[−] cells than actually may be best equipped for metastatic spread. Importantly, we observed trends linking the high abundance of well mechanically fit CTCs with high enumeration of all co-purified macrophages. Preferences of CTCs with particular nanomechanical phenotypes to coisolate with macrophages of certain polarizations may indicate specific strategies used by CTCs to survive and enhance metastatic potential. We also noted a similar association of CTCs mechanical properties and enumeration of macrophages for patients with liver, pancreatic, and lung cancer (Osmulski, Gaczynska, Huang, Taverna, Mahalingam, manuscript in preparation).

We did not detect a substantial correlation between mechanical fitness of CTCs and PSA levels or Gleason scores, consistently with our previous studies (8). In the cohort analyzed here, over 90% of cases were labeled as castration-sensitive at the time of the blood draw. However, the patients displayed diverse history of ADT. CTCs isolated from post-ADT patients, even those responding to AD, were generally

Macrophages Promote Aggressive Mechanical Phenotype of CTCs

**Figure 6.**

Subpopulations of prostate cancer DU145 cells cocultured with model macrophages (U937) display a hybrid EMT. **A**, GFP-DU145 were separated from macrophages in Cytobank and subjected to CyTOF analysis with an E/M panel of 16 antibodies (Supplementary Table S3). **B**, t-SNE projections of cocultured DU145 cells. Each of our cocultured populations was further divided into subpopulations. **C**, Profiles of selected epithelial and mesenchymal markers under distinct coculture conditions. **D**, Scatter plot of mesenchymal (M) and epithelial (E) indices under distinct coculture conditions. **E**, Violin plots of M/E ratio. **F**, Heatmap of oncogenic signal components of each cluster aligned on the basis of M/E ratio order.

well fit, likely reflecting the long course of disease in these patients. In turn, the presumed relations between CTCs and macrophages seemed to be more pronounced in pre-ADT than in post-ADT cases, highlighting necessity of tailoring different therapeutic approaches. For now, nanomechanical phenotypes and enumera-

tions of TACCs isolated from patients that remained CS for several months after analysis tend to cluster together, opening an attractive opportunity for predictive biomarking. Apart from castration resistance, our observation suggesting a trend linking the high adhesion of CTCs with the presence of metastatic disease may bear

a significant prognostic potential to be explored with longitudinal studies.

The correlations observed for patient-isolated TACCs obviously did not implicate causative relationships. However, our analysis of prostate cancer cells cocultured with model macrophages strongly suggested that macrophages might instruct cancer cells to acquire mechanical fitness. Interestingly, it was reported that macrophages engaged in cell–cell interactions may respond to mechanical clues in a similar manner to canonical ligand–receptor stimuli (39). This opens a possibility of functionally relevant mechanical cross-influence of both types of cells. The static conditions selected for model coculture did not include fluid shear stress and thus would correspond to preinvasation interactions between TAMs and future-CTCs. The strongest shift observed in the model coculture was an increase in cancer cells' adhesion in an apparent partial reversal of EMT. The sole exception with a significant decrease in adhesion was observed for 22Rv1 cells cocultured with M2-like macrophages. The diverse 22Rv1 cells may use the specific macrophage-mediated boost to advance EMT, increase softness and decrease adhesion before the CTC-specific partial EMT reversal. The partial reversal of EMT in model tumor cells cocultured with macrophages was confirmed by proteomic studies. However, mesenchymal and epithelial markers responded distinctly to particular types of macrophages, likely signaling multiple E/M states. Indeed, the significance of context-dependent EMP for cancer-relevant processes, including CTC invasiveness, is increasingly being acknowledged (5). In turn, the enhanced adhesive properties of cancer cells have been recently recognized as crucial for efficient cell survival and dissemination (40, 41). In our previous works we demonstrated mechanistic links between EMT signaling and cells' mechanical properties (9, 22, 23). Our data add to the notion of diversity of EMTs and point at the mechanical phenotype as the robust functional readout aligned with the cancer cells' destiny.

Multiple observations in patients, animal and cell culture models support the metastasis-promoting role of TAMs (4, 31, 42, 43), including induction of EMT (42, 43) and help in intravasation (4, 44, 45). We demonstrate that specific modulation of mechanical properties is the critical part of TAM-CTC relationship.

Here we propose that TAMs coach selected tumor cells to reach a distinctive stage of EMT characterized by high softness and high adhesion, with a mix of epithelial and mesenchymal molecular markers. Selection of tumor cells can be based in part on mechanical cues affecting cells subjected to in-tumor pressure (Qian, Osmulski, Gaczynska; manuscript in preparation). The phenotype of intermediate E/M state and mechanical fitness is critical for early survival of CTCs. Adhesive CTCs may intravasate as large survival-supporting clusters called circulating tumor microemboli (CTM; refs. 4, 14). TAMs may accompany CTCs and continue to help them as a part of CTMs or smaller clusters. An extreme form of assistance from macrophages would be formation of invasive CTC–macrophage fusions (46). Among the diverse microfiltration-isolated TACCs we noted putative fused cells, not included in our enumerations and beyond the scope of this study. The adhesive CTCs may also recruit other cells. For example, platelets may protectively coat CTCs, promote EMT and finally support extravasation (16). MDSCs found in tumor environment and in circulation (47–49), can cluster with CTCs, shield them and promote mitogenesis (17). In turn, CTC–neutrophil interactions stimulate cell-cycle progression and extravasation (18, 50). Without any apparent assistance from other types of cells, single

CTCs may still survive blood circulation, if they can assume a particular stiff-deformable phenotype similar to erythrocytes. We found such CTCs abundant in patients' blood. We speculate that these nonadhesive and spherical cells have limited capability to invade unless they can establish interactions with other circulating cells.

Summarizing our and others data from the life journey of CTCs, we envision the following metastasis-promoting chain of events. TAMs coach CTCs for mechanical endurance and propensity to cluster, help them to intravasate and accompany them as chaperones in the blood. CTCs use the high adhesiveness to keep integrity of microemboli and for abundant cell–cell interactions. All cells clustered with CTCs act as shields from fluid shear stress and leukocyte attacks. Platelets, MDSCs, and neutrophils additionally help in later stages of CTC life, restarting EMT and proliferation and enabling extravasation. This chain of events from intra- to extravasation and metastatic growth would not be possible without the macrophage-promoted EMP and mechanical fitness of CTCs.

Authors' Disclosures

P.A. Osmulski reports a patent for HSC-1697 provisional pending to The Board of Regents of the UT System and a patent for HSC-1572 provisional pending to The Board of Regents of the UT. D. Mahalingam reports personal fees from Amgen, Eisai, Exelixis, and Bristol Myers Squibb, and grants from Merck and Oncolytics outside the submitted work. M.E. Gaczynska reports a patent for HSC-1697 provisional pending to The Board of Regents of the UT System and a patent for HSC-1572 provisional pending to The Board of Regents of the UT System. No disclosures were reported by the other authors.

Authors' Contributions

P.A. Osmulski: Conceptualization, data curation, formal analysis, supervision, funding acquisition, validation, investigation, visualization, methodology, writing—original draft, project administration, writing—review and editing. **A. Cunsolo:** Validation, investigation, visualization, methodology, writing—review and editing. **M. Chen:** Validation, investigation, visualization, methodology. **Y. Qian:** Validation, investigation, visualization. **C.-L. Lin:** Data curation, software, formal analysis, visualization, methodology. **C.-N. Hung:** Formal analysis, investigation, visualization, methodology, writing—review and editing. **D. Mahalingam:** Resources, writing—review and editing. **N.B. Kirma:** Resources, formal analysis, investigation, methodology. **C.-L. Chen:** Investigation, methodology. **J.A. Taverna:** Methodology, writing—review and editing. **M.A. Liss:** Conceptualization, resources, writing—review and editing. **I.M. Thompson:** Resources. **T. H.-M. Huang:** Conceptualization, resources, supervision, funding acquisition, methodology, project administration, writing—review and editing. **M.E. Gaczynska:** Conceptualization, formal analysis, supervision, validation, investigation, visualization, methodology, writing—original draft, project administration, writing—review and editing.

Acknowledgments

This work was supported by U.S. Department of Defense grant PC170821 [T. H.-M. Huang (principal investigator), P.A. Osmulski, M.E. Gaczynska, M. Chen, Y. Qian, C.-L. Lin, and C.-N. Hung], NIH U54 CA217297-01 [P.A. Osmulski (principal investigator) and A. Cunsolo], and William and Ella Owens Medical Research Foundation [M.E. Gaczynska and P.A. Osmulski (principal investigators)]. The authors acknowledge the assistance of the Bioanalytics and Single-Cell Core (BASiC) for atomic force microscopy and mass cytometry studies, in part supported by the Cancer Prevention & Research Institute of Texas (CPRI) award RP150600 [to T. H.-M. Huang (principal investigator), N.B. Kirma, and P.A. Osmulski].

The costs of publication of this article were defrayed in part by the payment of page charges. This article must therefore be hereby marked *advertisement* in accordance with 18 U.S.C. Section 1734 solely to indicate this fact.

Received October 25, 2020; revised April 6, 2021; accepted May 25, 2021; published first May 27, 2021.

References

- Micalizzi DS, Maheswaran S, Haber DA. A conduit to metastasis: circulating tumor cell biology. *Genes Dev* 2017;31:1827–40.
- Jin K, Chen X, Lan H, Wang S, Ying X, Abdi SM, et al. Current progress in the clinical use of circulating tumor cells as prognostic biomarkers. *Cancer Cytopathol* 2019;127:739–49.
- Follain G, Herrmann D, Harlepp S, Hyenne V, Osmani N, Warren SC, et al. Fluids and their mechanics in tumour transit: shaping metastasis. *Nat Rev Cancer* 2020;20:107–24.
- Katt ME, Wong AD, Searson PC. Dissemination from a solid tumor: examining the multiple parallel pathways. *Trends Cancer* 2018;4:20–37.
- Yang J, Antin P, Berx G, Blanpain C, Brabletz T, Bronner M, et al. Guidelines and definitions for research on epithelial–mesenchymal transition. *Nat Rev Mol Cell Biol* 2020;21:341–52.
- Stroka KM, Konstantopoulos K. Physical Biology in Cancer. 4. Physical cues guide tumor cell adhesion and migration. *AJP Cell Physiol* 2014;306:C98–109.
- Chen CL, Mahalingam D, Osmulski P, Jadhav RR, Wang CM, Leach RJ, et al. Single-cell analysis of circulating tumor cells identifies cumulative expression patterns of EMT-related genes in metastatic prostate cancer. *Prostate* 2013;73:813–26.
- Osmulski P, Mahalingam D, Gaczynska ME, Liu J, Huang S, Horning AM, et al. Nanomechanical biomarkers of single circulating tumor cells for detection of castration resistant prostate cancer. *Prostate* 2014;74:1297–307.
- Huang G, Osmulski PA, Bouamar H, Mahalingam D, Lin CL, Liss MA, et al. TGF- β signal rewiring sustains epithelial–mesenchymal transition of circulating tumor cells in prostate cancer xenograft hosts. *Oncotarget* 2016;7:77124–37.
- Cross SE, Jin YS, Rao J, Gimzewski JK. Applicability of AFM in cancer detection. *Nat Nanotechnol* 2009;4:72–3.
- Zemora J, Danilkiewicz J, Orzechowska B, Pabijan J, Seweryn S, Lekka M. Atomic force microscopy as a tool for assessing the cellular elasticity and adhesiveness to identify cancer cells and tissues. *Semin Cell Dev Biol* 2018;73:115–24.
- Rejniak KA. Circulating tumor cells: when a solid tumor meets a fluid micro-environment. *Adv Exp Med Biol* 2016;936:93–106.
- Lamouille S, Xu J, Derynck R. Molecular mechanisms of epithelial–mesenchymal transition. *Nat Rev Mol Cell Biol* 2014;15:178–96.
- Aceto N, Bardia A, Miyamoto DT, Donaldson MC, Wittner BS, Spencer JA, et al. Circulating tumor cell clusters are oligoclonal precursors of breast cancer metastasis. *Cell* 2014;158:1110–22.
- Heeke S, Mograbi B, Alix-Panabières C, Hofman P. Never travel alone: the crosstalk of circulating tumor cells and the blood microenvironment. *Cells* 2019;8:714.
- Leblanc R, Peyruchaud O. Metastasis: new functional implications of platelets and megakaryocytes. *Blood* 2016;128:24–31.
- Sproule ML, Welte T, Boral D, Liu HN, Yin W, Vishnoi M, et al. PMN-MDSCs enhance CTC metastatic properties through reciprocal interactions via ROS/Notch/Nodal signaling. *Int J Mol Sci* 2019;20:1916.
- Szczerba BM, Castro-Giner F, Vetter M, Krol I, Gkoutela S, Landin J, et al. Neutrophils escort circulating tumour cells to enable cell cycle progression. *Nature* 2019;566:553–7.
- Adams DL, Martin SS, Alpaugh RK, Charpentier M, Tsai S, Bergan RC, et al. Circulating giant macrophages as a potential biomarker of solid tumors. *Proc Natl Acad Sci U S A* 2014;111:3514–9.
- Chen M, Pereira-Smith OM, Tominaga K. Loss of the chromatin regulator MRG15 limits neural stem/progenitor cell proliferation via increased expression of the p21 Cdk inhibitor. *Stem Cell Res* 2011;7:75–88.
- Genin M, Clement F, Fattaccioli A, Raes M, Michiels C. M1 and M2 macrophages derived from THP-1 cells differentially modulate the response of cancer cells to etoposide. *BMC Cancer* 2015;15:577.
- Hsu YT, Osmulski P, Wang Y, Huang YW, Liu L, Ruan J, et al. EpCAM-regulated transcription exerts influences on nanomechanical properties of endometrial cancer cells that promote epithelial-to-mesenchymal transition. *Cancer Res* 2016;76:6171–82.
- Taverna JA, Hung CN, DeArmond DT, Chen M, Lin CL, Osmulski PA, et al. Single-cell proteomic profiling identifies combined AXL and JAK1 inhibition as a novel therapeutic strategy for lung cancer. *Cancer Res* 2020;80:1551–63.
- Truong M, Yang B, Jarrard DF. Toward the detection of prostate cancer in urine: a critical analysis. *J Urol* 2013;189:422–9.
- Nikolaev NI, Müller T, Williams DJ, Liu Y. Changes in the stiffness of human mesenchymal stem cells with the progress of cell death as measured by atomic force microscopy. *J Biomech* 2014;47:625–30.
- Downey GP, Doherty DE, Schwab B, Elson EL, Henson PM, Worthen GS. Retention of leukocytes in capillaries: role of cell size and deformability. *J Appl Physiol* 1990;69:1767–78.
- Armstrong AJ, Marengo MS, Oltean S, Kemeny G, Bittling RL, Turnbull JD, et al. Circulating tumor cells from patients with advanced prostate and breast cancer display both epithelial and mesenchymal markers. *Mol Cancer Res* 2011;9:997–1007.
- Ambarus CA, Krausz S, van Eijk M, Hamann J, Radstake TRDJ, Reedquist KA, et al. Systematic validation of specific phenotypic markers for in vitro polarized human macrophages. *J Immunol Methods* 2012;375:196–206.
- Shabo I, Stål O, Olsson H, Doré S, Svanvik J. Breast cancer expression of CD163, a macrophage scavenger receptor, is related to early distant recurrence and reduced patient survival. *Int J Cancer* 2008;123:780–6.
- Cao W, Peters JH, Nieman D, Sharma M, Watson T, Yu J. Macrophage subtype predicts lymph node metastasis in oesophageal adenocarcinoma and promotes cancer cell invasion in vitro. *Br J Cancer* 2015;113:738–46.
- Lin Y, Xu J, Lan H. Tumor-associated macrophages in tumor metastasis: biological roles and clinical therapeutic applications. *J Hematol Oncol* 2019;12:76.
- Shrivastava R, Shukla N. Attributes of alternatively activated (M2) macrophages. *Life Sci* 2019;224:222–31.
- Wang Q, Ni H, Lan L, Wei X, Xiang R, Wang Y. Fra-1 protooncogene regulates IL-6 expression in macrophages and promotes the generation of M2 macrophages. *Cell Res* 2010;20:701–12.
- Murray PJ. Macrophage polarization. *Annu Rev Physiol* 2017;79:541–66.
- Li J, Alvero AB, Nuti S, Tedja R, Roberts CM, Pitruzzello M, et al. CBX7 binds the E-box to inhibit TWIST-1 function and inhibit tumorigenicity and metastatic potential. *Oncogene* 2020;39:3965–79.
- Ballermann BJ, Dardik A, Eng E, Liu A. Shear stress and the endothelium. *Kidney Int* 1998;54:S100–8.
- Deng Y, Papageorgiou DP, Chang HY, Abidi SZ, Li X, Dao M, et al. Quantifying shear-induced deformation and detachment of individual adherent sickle red blood cells. *Biophys J* 2019;116:360–71.
- Khismatullin DB. The cytoskeleton and deformability of white blood cells. In: Ley K, editor. *Leukocyte rolling and adhesion: current topics in membranes*. Vol. 64. New York: Academic Press; 2009. p. 47–111.
- Patel NR, Bole M, Chen C, Hardin CC, Kho AT, Mih J, et al. Cell elasticity determines macrophage function. *PLoS One* 2012;7:e41024.
- Janiszewska M, Primi MC, Izard T. Cell adhesion in cancer: beyond the migration of single cells. *J Biol Chem* 2020;295:2495–505.
- Kim H, Ishibashi K, Matsuo K, Kira A, Okada T, Watanabe K, et al. Quantitative measurements of intercellular adhesion strengths between cancer cells with different malignancies using atomic force microscopy. *Anal Chem* 2019;91:10557–63.
- Su S, Liu Q, Chen J, Chen J, Chen F, He C, et al. A positive feedback loop between mesenchymal-like cancer cells and macrophages is essential to breast cancer metastasis. *Cancer Cell* 2014;25:605–20.
- Wei C, Yang C, Wang S, Shi D, Zhang C, Lin X, et al. Crosstalk between cancer cells and tumor associated macrophages is required for mesenchymal circulating tumor cell-mediated colorectal cancer metastasis. *Mol Cancer* 2019;18:64.
- Roussos ET, Condeelis JS, Patsialou A. Chemotaxis in cancer. *Nat Rev Cancer* 2011;11:573–87.
- Harney AS, Arwert EN, Entenberg D, Wang Y, Guo P, Qian BZ, et al. Real-time imaging reveals local, transient vascular permeability, and tumor cell intravasation stimulated by TIE2hi macrophage-derived VEGFA. *Cancer Discov* 2015;5:932–43.
- Gast CE, Silk AD, Zarour L, Riegler L, Burkhart JG, Gustafson KT, et al. Cell fusion potentiates tumor heterogeneity and reveals circulating hybrid cells that correlate with stage and survival. *Sci Adv* 2018;4:eaat7828.
- Porta C, Sica A, Riboldi E. Tumor-associated myeloid cells: new understandings on their metabolic regulation and their influence in cancer immunotherapy. *FEBS J* 2018;285:717–33.
- Yang L, Huang J, Ren X, Gorska AE, Chytil A, Aakre M, et al. Abrogation of TGF β signaling in mammary carcinomas recruits Gr-1+CD11b+ myeloid cells that promote metastasis. *Cancer Cell* 2008;13:23–35.
- Du R, Lu KV, Petritsch C, Liu P, Ganss R, Passequé E, et al. HIF1 α induces the recruitment of bone marrow-derived vascular modulatory cells to regulate tumor angiogenesis and invasion. *Cancer Cell* 2008;13:206–20.
- Spicer JD, McDonald B, Cools-Lartigue JJ, Chow SC, Giannias B, Kubas P, et al. Neutrophils promote liver metastasis via Mac-1-mediated interactions with circulating tumor cells. *Cancer Res* 2012;72:3919–27.

Cancer Research

The Journal of Cancer Research (1916–1930) | The American Journal of Cancer (1931–1940)

Contacts with Macrophages Promote an Aggressive Nanomechanical Phenotype of Circulating Tumor Cells in Prostate Cancer

Pawel A. Osmulski, Alessandra Cunsolo, Meizhen Chen, et al.

Cancer Res 2021;81:4110-4123. Published OnlineFirst May 27, 2021.

Updated version Access the most recent version of this article at:
doi:[10.1158/0008-5472.CAN-20-3595](https://doi.org/10.1158/0008-5472.CAN-20-3595)

Supplementary Material Access the most recent supplemental material at:
<http://cancerres.aacrjournals.org/content/suppl/2021/05/27/0008-5472.CAN-20-3595.DC1>

Cited articles This article cites 50 articles, 9 of which you can access for free at:
<http://cancerres.aacrjournals.org/content/81/15/4110.full#ref-list-1>

E-mail alerts [Sign up to receive free email-alerts](#) related to this article or journal.

Reprints and Subscriptions To order reprints of this article or to subscribe to the journal, contact the AACR Publications Department at pubs@aacr.org.

Permissions To request permission to re-use all or part of this article, use this link <http://cancerres.aacrjournals.org/content/81/15/4110>. Click on "Request Permissions" which will take you to the Copyright Clearance Center's (CCC) Rightslink site.